FACULTY OF SCIENCE AND TECHNOLOGY

MASTER THESIS

Study programme / specialisation:
Mechanical and Structural Engineering and Materials Science / Civil Engineering Structures

The spring semester, 2022

Open / Confidential

Author: Cristina Tawede Besin

……
(author's signature)

Course coordinator: Sudath C. Siriwardane

Supervisor(s): Ashish Aeran

Thesis title: Global Fatigue Analysis of the Mooring Systems for Offshore Floating Structures

Credits (ECTS): 30

Keywords:
Mooring system
Offshore floating structures
Global fatigue analysis
Fatigue life
Fatigue damage
FPSO
Wave frequency
Low frequency

Pages: 56

+ appendix: 4

Stavanger, 15.06.2022

Acknowledgement

I express my most profound appreciation to my supervisor, Associate Professor Ashish Aeran. Without his support, guidance, and feedback, this master thesis would have been impossible.

I am also grateful to my peers, Usman Shaukat and Navaneethan Kurukkal, for their help with the software and insightful comments and suggestions.

Lastly, I want to thank my family for their unwavering support. Their encouraging words have kept my spirits and motivation high during this journey.

Abstract

The mooring system is essential for keeping the floating structures in place while performing marine applications under adverse weather conditions. However, mooring systems are subjected to fluctuating stresses due to structural details, material characteristics, and environmental factors resulting in fatigue damage. In addition, most studies only perform a local fatigue analysis focusing on the upper chain. However, a global fatigue assessment is necessary to determine the most critical fatigue location along the mooring line. A turret moored FPSO with nine mooring lines in a 400-meter water depth is utilised in this study. The metocean data is taken from the Gulf of Mexico. Three different mooring system designs have been established to analyse further the global fatigue analysis of the mooring lines induced by low frequency, wave frequency, and combined responses. Results reveal that the fatigue damage of the moorings is greatly influenced by wave frequency motion, and the chain at fairleads is the most critical fatigue location for all three cases. Conversely, the least critical fatigue location is the chain at the top of the bottom chain in case 1, while it is the chain at the seabed interaction point in cases 2 and 3. Results also show that the chain-polyester-chain system has more extended fatigue life than chain-chain-chain and chain-wire-chain systems. This paper also provides further recommendations for future work.

Keywords: *mooring system, offshore floating structures, global fatigue analysis, fatigue life, FPSO, wave frequency, low frequency*

Table of Contents

List of Figures

List of Figures

List of Tables

Nomenclature

Latin Characters

A_5	elongation
A_γ	normalising factor
a_D	intercept of the S-N curve
B	breadth of the vessel
C_b	block coefficient
D	annual cummulative fatigue damage ratio
d	nominal diameter
f	frequency
GM_l	longitudinal metacentric height
GM_t	transverse metacentric height
H	height of the vessel
H_s	significant wave height
$I_u(z)$	turbulence intensity
i	tension range interval
K	intercept of the T-N curve
L	fatigue life
L_m	ratio of mean load to reference breaking strength
M	slope of the T-N curve
m	slope of the S-N curve
N	number of cycles of the T-N curve
n	number of load steps
$n_c(s)$	number of cycles of the S-N curve
N_i	number of cycles to failure at normalised tension range
n_i	number of cycles per year within the tension range interval
R3	chain quality according to IACS
R3S	chain quality according to IACS
R4	chain quality according to IACS

R4S	chain quality according to IACS
R5	chain quality according to IACS
R_e	yield stress
R_m	tensile strength
$S_{API}(f)$	American Petroleum Institute spectrum
$S_{NPD}(f)$	Norwegian Petroleum Directorate spectrum
$S_{PM}(\omega)$	Pierson-Moskowitz spectrum
$S(\omega)$	Ochi-Hubble spectrum
s	stress range (double amplitude)
T_p	peak wave period
t	wind speed averaging time
t_0	3600 seconds
U_0	1-hour mean wind speed at 10 meters above the water surface
$U(z)$	1-hour mean wind speed
$U(z,t)$	characteristic wind velocity
$V_{c_{wind}}$	wind-generated current velocity
Z	area reduction
z	height above the water surface
z_R	reference elevation

Greek Characters

Δ	displacement
γ	non-dimensional peak shape parameter
λ_s	shape factor
σ	spectral width parameter
ω	wave frequency
ω_p	spectral peak frequency

Abbreviations

ALS	accident limit state
API	American Petroleum Institute
CALM	catenary anchor leg platform
COG	centre of gravity
FLS	fatigue limit state
FPS	floating production system
FPSO	floating production, storage, and offloading unit
GOM	Gulf of Mexico
HMPE	high modulus polyethylene
IACS	International Association of Classification Societies
IWRC	independent wire rope core
JONSWAP	Joint North Sea Wave Project
LF	low frequency
MBS	minimum breaking strength
MODU	mobile offshore drilling unit
NPD	Norwegian Petroleum Directorate
OWA	Offshore West Africa
PM	Pierson-Moskowitz
RBS	reference breaking strength
SALM	single anchor leg mooring
SPM	single point mooring
TLP	tension leg platform
TTR	top tensioned riser
ULS	ultimate limit state
VIM	vortex-induced motion
VIV	vortex-induced vibration
WF	wave frequency
WSC	wire-strand core

Chapter 1 Introduction

This chapter presents the background of the study, objectives, theoretical basis on which this study is anchored, and the scope of work.

1.1 Background

The mooring system anchors the offshore floating structures to the seabed while conducting marine applications, such as drilling, production, and wind power generation under various environmental conditions. The mooring system components are mooring lines, connectors, and anchoring points. The mooring lines are typically chains, wire rope, fibre rope, or a combination of chains and wire or fibre ropes.

Fatigue plays a vital role in the design and analysis of the mooring system, as studies reveal that it is one of the primary reasons mooring lines fail. In addition, some research shows that the fairlead chain is often the most critical fatigue location of the mooring line, thus having the shortest fatigue life. As a result, most studies only perform a local fatigue analysis focusing on the upper chain. However, it is requisite to conduct a global fatigue assessment to determine the most critical fatigue location along the mooring line.

1.2 Objectives

The main objective of this thesis is to execute global fatigue damage and fatigue life calculation of the mooring lines. The detailed objectives are outlined below.

1. Establish three cases, with each having different mooring line components.
2. Perform a global fatigue analysis of the mooring system.
3. Determine the most critical fatigue location along the mooring line.
4. Find out the most critical mooring line based on the mooring system arrangement.
5. Calculate the fatigue life of the mooring lines.
6. Select the best mooring component layout for the given sea state.

1.3 Theoretical Basis

This study is conducted to connect with the research of Wu et al. [1] about the governing factors and locations of fatigue damage on mooring lines of floating structures. Wu et al. [1] conducted an analytical analysis of the chain-polyester-chain mooring line focusing on the low frequency (LF) and wave frequency (WF) responses. A semi-submersible platform with metocean parameters from the Gulf of Mexico (GOM) and Offshore West Africa (OWA) is used in the study. It is found that the lower section of a mooring line near the seabed appears to be the location of the most critical fatigue damage induced by LF motion. On the other hand, the WF fatigue damage may occur at the moorings' fairlead or bottom section.

Furthermore, Wu et al. [1] emphasise that the critical fatigue locations may differ due to mooring configuration, component layout, metocean criteria, and floating structure. Therefore, this present study carries out a global fatigue evaluation of a mooring line in GOM with a different mooring arrangement, configuration, and floating platform to determine the critical fatigue damage location and the fatigue life of the mooring system.

1.4 Scope of Work

This study focuses on the global fatigue analysis of the mooring lines to distinguish its critical fatigue points and fatigue life induced by different responses. This study consists of eight chapters.

1. Chapter 1 introduces the background and the purpose of this study.
2. A literature review of the different offshore floating structures presently used in the industry is discussed in Chapter 2.
3. Chapter 3 presents a literature review of the mooring systems.
4. A brief overview of offshore riser systems is tackled in Chapter 4.
5. A review of the fatigue analysis and the environmental loads and conditions for which a mooring system should be assessed are explained in Chapter 5.
6. The three case studies of mooring system designs and their parameters are presented in Chapter 6.
7. The global fatigue analysis results are thoroughly studied and explained in Chapter 7.
8. Chapter 8 presents the conclusions and proposals based on the observed results.

Chapter 2 Floating Offshore Structures

Offshore structures are predominantly used for the exploration and production of oil and gas. These structures are divided into two main categories, fixed and floating [2]. Fixed platforms and compliant towers were initially used. However, these structures are bottom-supported and are limited to a water depth of about 300 to 1500 meters. On the other hand, floating structures built for exploration and production have become popular because of significant oil and gas fields discoveries in deeper and more distant locations [3]. Therefore, this chapter introduces the four types of floating structures that are particularly suited for deepwater applications.

2.1 Tension Leg Platform (TLP)

The tension leg platform, so-called TLP, is a floating structure permanently anchored to the seabed through tendons that provide stability. Halkyard [4] mentions that TLP can be used for production, drilling, and workover operations but does not provide storage. It consists of columns, pontoons, deck, hull, and mooring systems, as shown in Figure 2-1. The mooring systems are comprised of tendons that are groups of tethers made of high-strength steel pipes. The axial stiffness of the tendons restricts the vertical plane motions such as pitch, roll, and heave. On the other hand, the tendon pre-tension allows horizontal plane motions, including yaw, sway, and surge [2].

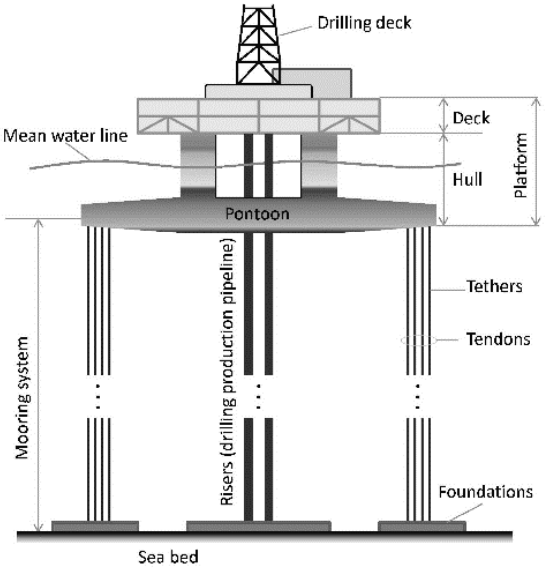

Figure 2-1 An example of TLP [5]

Furthermore, Halkyard [4] highlights that one of the most critical components of TLP is the hull, as it provides buoyancy both for the support of weight and for giving tendon tensions. Payloads and tendon tension considerably affect the size of the hull. Therefore, the hull must be tall enough to provide wave clearance to the deck in every operation.

Some of the advantages of TLP are low operating costs and reduced maintenance costs. The other three floating structures have no limitation in water depth. However, TLP is restricted because it is costly when the location goes deeper. In addition, it cannot be moved from one place to another as a permanently sited platform compared to the other floating structures [4].

2.2 Surface Piercing Articulated Riser (Spar)

Spar is a floating offshore platform supporting wet and dry trees in extensive deepwater drilling and production applications. Different types of spar have been discovered as technology progressed over time. Classic spar, cell spar, and truss spar are the ones that exist today. Among them, the truss spar is widely used [6]. Figure 2-2 refers to the inboard and outboard classic spar and outward truss spar.

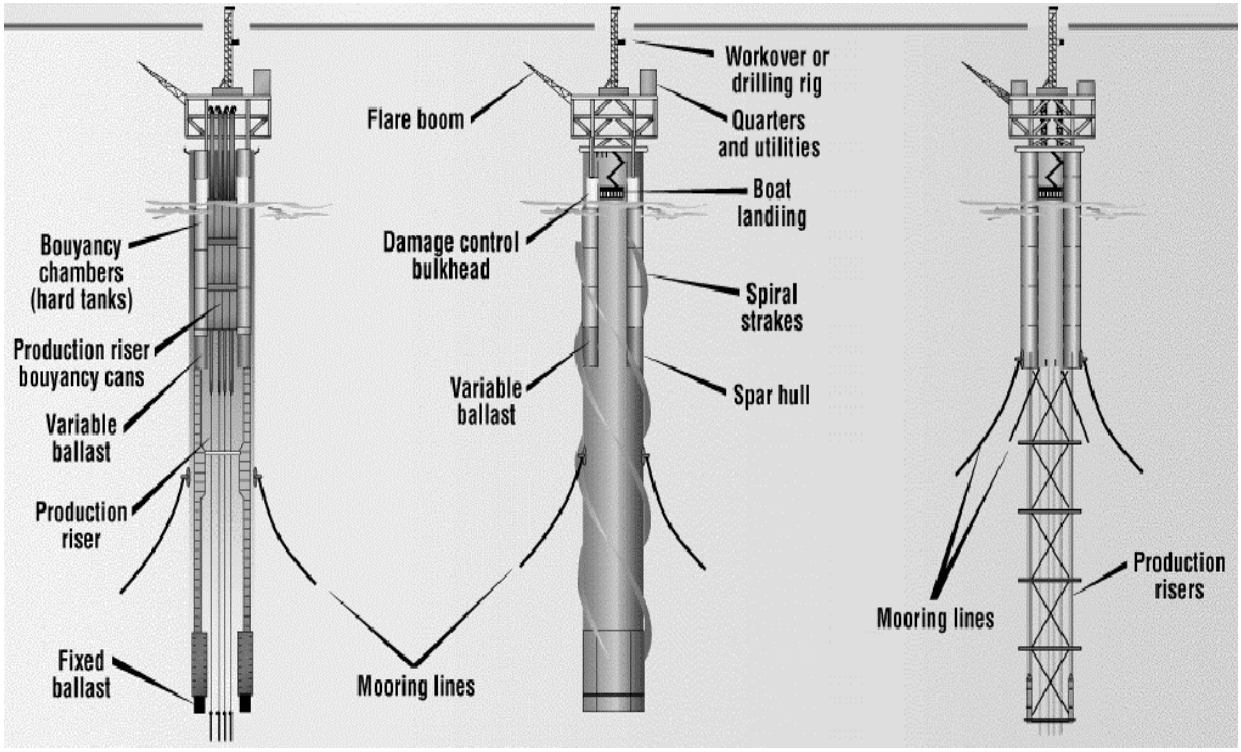

Figure 2-2 The inboard classic, outward classic, and outward truss spar (left to right) [7]

Halkyard [4] states that the spar has a very deep draft and a moderate to small waterplane area. Also, it can be utilised for production, storage, drilling, and workover operations. Identical to TLP, the spar has also limitations in its motions. However, the centre of gravity must be placed below the centre of buoyancy to attain the spar's stability. Ma et al. [3] mention that a spar typically uses a spread mooring system with nine or 12 mooring lines grouped into three connected from the outer shell of the platform to the seafloor.

Furthermore, the spar comprises a deck, hard and soft tanks, and a midsection. The deck is supported by four columns attached to the hard tank at the intersection of a radial bulkhead with the outer shell. The midsection extends below the hard tank to provide the spar with its deep draft. The hard tank provides the buoyancy to support the deck, ballast, hull, and vertical tensions. The soft tank is located at the bottom of the spar and usually provides buoyancy during the installation phases when the spar is floating horizontally [4].

According to API RP 2SK [8], cylindrical structures like spar, TLP, and semi-submersibles may experience vortex-induced motion (VIM) when exposed to currents. However, studies show that TLP and semis, as multi-column floaters, only experience limited VIM. Therefore, the spar is the most distinguished floating platform susceptible to VIM.

2.3 Semisubmersible (Semi)

Semisubmersible is a stable, cost-effective platform for drilling, oil production, heavy lifting, and accommodation [3]. The spacious deck is supported by pontoon-type columns immersed in the water. Semisubmersible is generally used as the offshore industry moves farther and deeper in water locations due to its ability to withstand harsh environmental conditions. Furthermore, its floatation stability is derived from the columns. In contrast to spar, the centre of gravity of the semi is above the centre of buoyancy [9].

Halkyard [4] describes pontoons, stability columns, deck, and space frame bracing as the main components of a semi-submersible determined by its transverse strength system. An illustration of a semi-submersible is presented in Figure 2-3. It has a small waterplane area and a moderate draft. The mooring system typically comprises 12 or 16 mooring lines grouped into four secured from the four columns to the seafloor [3].

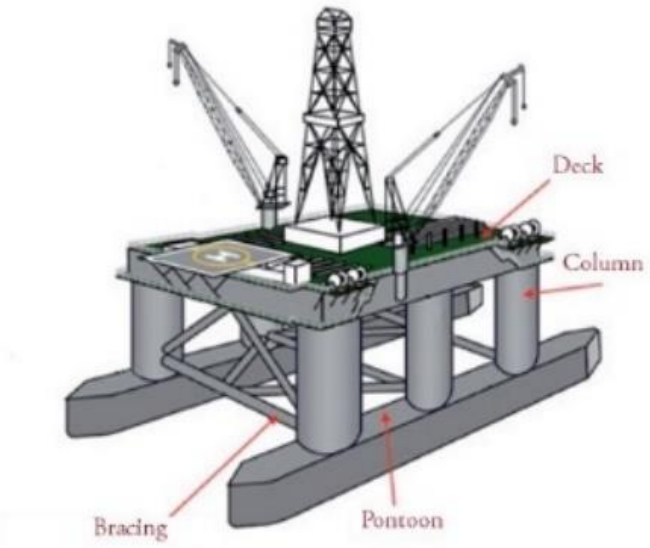

Figure 2-3 A semi-submersible model [10]

2.4 Floating Production Storage and Offloading (FPSO)

Floating production storage and offloading, also known as FPSO, is a ship-shaped vessel with a shallow draft and a large waterplane. FPSO provides processing equipment and storage for hydrocarbons and crude oil. First, it receives fluids from a subsea reservoir through risers, separating them into crude oil, natural gas, water, and impurities. Then, the stored crude oil is offloaded onto shuttle tankers to go to market or for further refining onshore [11]. A typical FPSO with an internal turret is represented in Figure 2-4, while Figure 2-5 illustrates the subsea facilities of an FPSO.

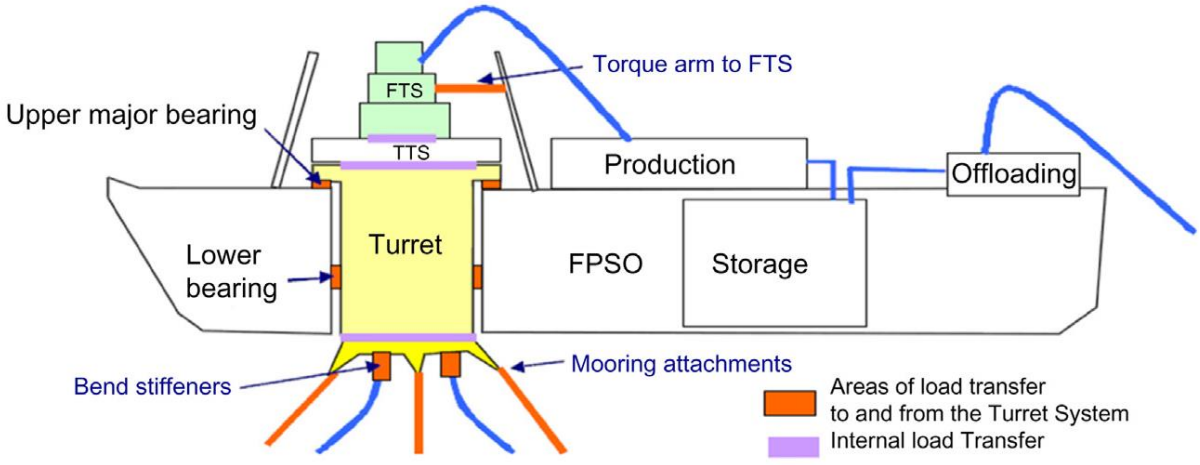

Figure 2-4 A typical FPSO [12]

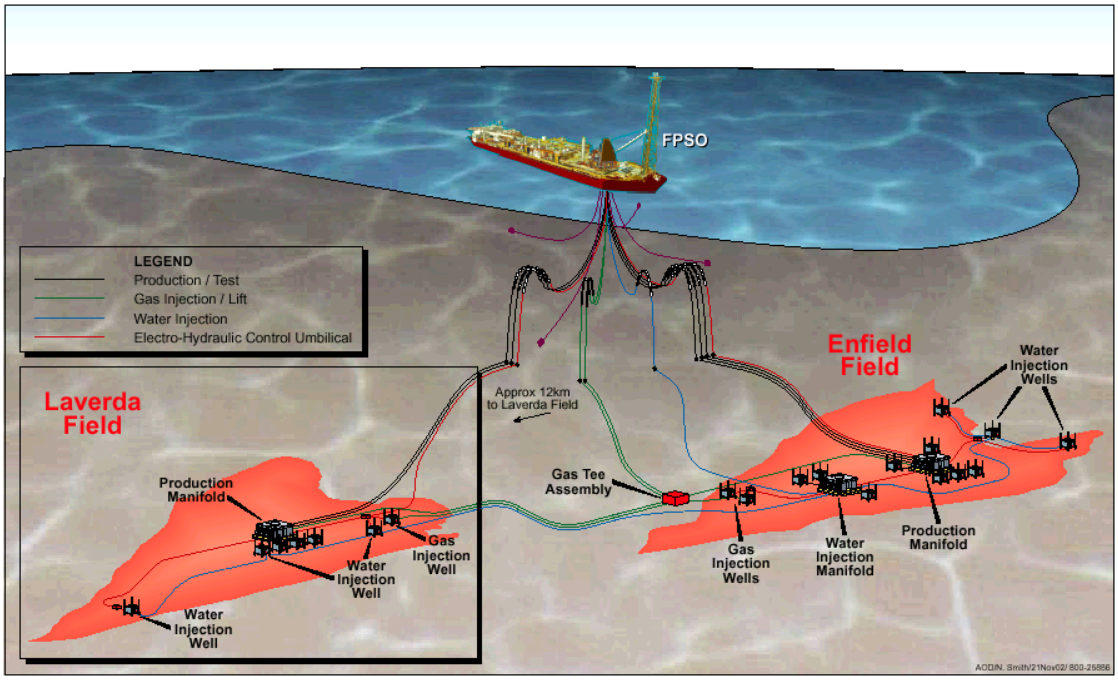

Figure 2-5 The typical FPSO subsea facilities [12]

FPSOs use internal or external turret mooring systems, effective in deeper and harsher environments. A disconnectable turret is also an excellent option when the location is prone to hurricanes and typhoons. Thus, the FPSOs can be easily moved to a safer location, as illustrated in Figure 2-6.

Further, Mitra [9] states that FPSO is neutrally buoyant as it has six degrees of freedom. Mueller [13] also refers to the six degrees of freedom as angular and linear movements. The former denotes the three rotations like, pitch, roll and yaw, while the latter describes the displacements, including surge, sway, and heave.

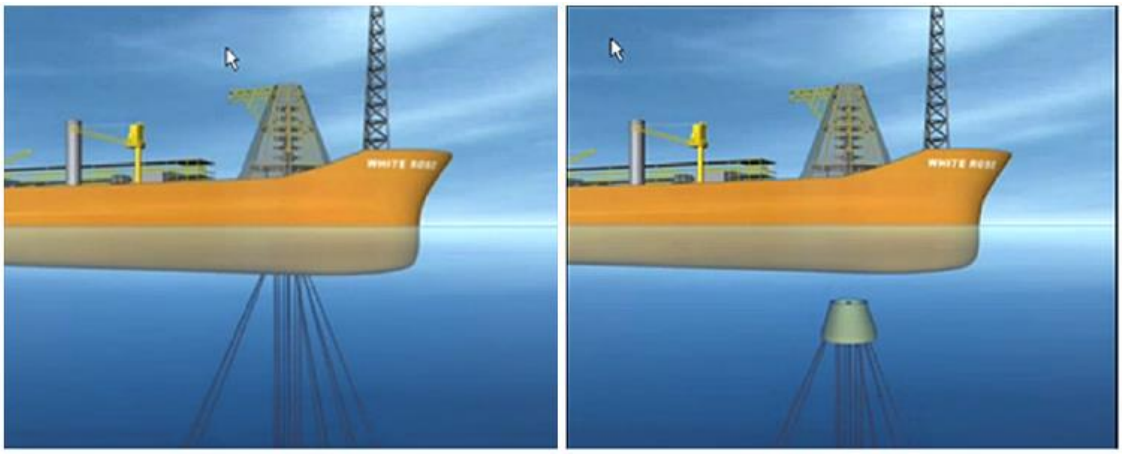

Figure 2-6 A disconnectable turret [3]

Chapter 3 Offshore Mooring Systems

The mooring systems are composed of mooring lines, anchors, and connectors. Its primary function is to hold floating structures while conducting offshore operations under adverse environmental conditions. Such operations include production, drilling, and wind power generation. Moreover, this chapter discusses the two main categories of mooring systems. The different configurations and components of a mooring line are also discussed.

3.1 Permanent and Temporary Mooring Systems

A permanent mooring is also called a long-term mooring that provides station-keeping for a floating facility at the exact location for more than five years [14]. This type of mooring is practically utilised in oil and gas production activities. It usually has a design life of 25 years. Hence, fatigue analysis must be performed. On the contrary, mobile mooring anchors a floating platform at the exact location for less than five years [14]. Thus, performing fatigue analysis is unnecessary. This type of mooring is used for drilling or accommodation rigs for performing offshore operations.

3.2 Mooring System Configurations

A mooring system is essential for keeping the floating structures in place while performing marine applications. Therefore, this section presents the different configurations of a mooring system.

3.2.1 Catenary Mooring

A catenary mooring has a typical free-hanging line with a part lying horizontally on the seabed, thus not having vertical forces at the anchor. The suspension of the weight of the mooring lines provides restoring forces on floating platforms. Thus, the mooring lengths must be longer than the water depth [15]. This mooring is typically used in shallow to medium-depth water. Figure 3-1 shows a typical example of catenary mooring [3].

The weight of the line controls the stiffness. As a result, stiffness swiftly increases as the line is being stretched. Moreover, the catenary system relies on the stiffness of the mooring components when the system is fully tensioned. Eventually, the system fails as loads increase quickly [16].

Furthermore, a catenary mooring system uses a combination of chain and wire. The chain must be placed at the bottom to control the restoring forces. However, increasing the length of the mooring lines also increases its weight, which lessens the vessel's working payloads as the water depth increases [17]. Therefore, a wire can replace some chains to reduce the weight of the moorings [16].

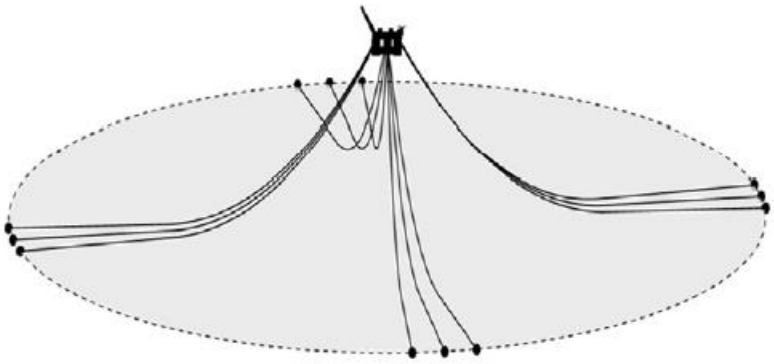

Figure 3-1 The catenary mooring system [3]

3.2.2 Taut Mooring

Contrary to the catenary mooring, taut mooring has no lines on the seabed as the lines are taut from the seafloor to the platform's fairlead. Thus, the mooring system consumes less line material and a smaller anchor footprint. However, this type of mooring is not applicable in shallow water as this may be too inelastic, thus increasing the tension of the line exceedingly. Therefore, taut mooring is more appropriate for deepwater use [3].

The taut mooring system often consists of lightweight wire or fibre ropes pre-tensioned until taut. Therefore, the catenary effect of a free-hanging line is insignificant. However, these lines have significant axial resistance and good fatigue properties. In addition, the elasticity of the fibre rope governs the restoring forces. The lines must have 30 to 40 degrees to the seabed at the anchor. Therefore, the anchor must be designed to resist both dynamic and static vertical forces. Figure 3-2 illustrates a taut mooring system [16, 17].

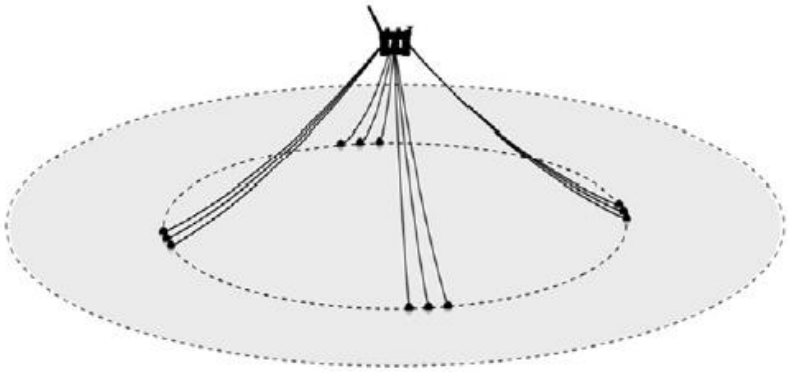

Figure 3-2 The taut mooring system [3]

3.2.3 Spread Mooring

The spread mooring system has numerous mooring lines positioned around the floating structure. Thus, it limits the platform's offset and heading once the anchors are deployed [3]. The arrangement of the lines must be symmetrical to hold the structure on its fixed heading location. However, this mooring restricts the unit to weathervane. Moreover, spread mooring is suitable for any water depth and offshore platform type [15]. Ma et al. [3] also emphasise that complicated rotational mechanical systems are not required as spread mooring is simple and economical. An example of spread mooring is illustrated in Figure 3-3.

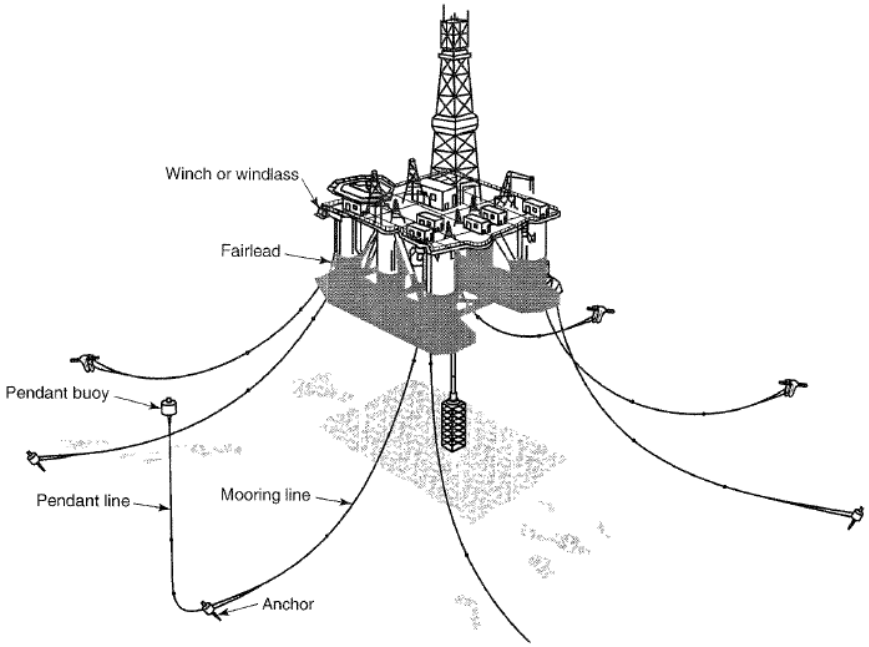

Figure 3-3 A typical spread mooring [8]

3.2.4 Single Point Mooring

A single-point mooring is often referred to as SPM. It is predominantly used for ship-shaped vessels like FPSOs, which are vulnerable to weather directions. This mooring reduces the wind, waves, and current loads, allowing the FPSO to weathervane [8]. However, SPM is difficult and costly to build [3]. A typical single-point mooring is demonstrated in Figure 3-4. Moreover, internal and external turret mooring systems, catenary anchor leg mooring (CALM), and single anchor leg mooring (SALM) are various types of SPM.

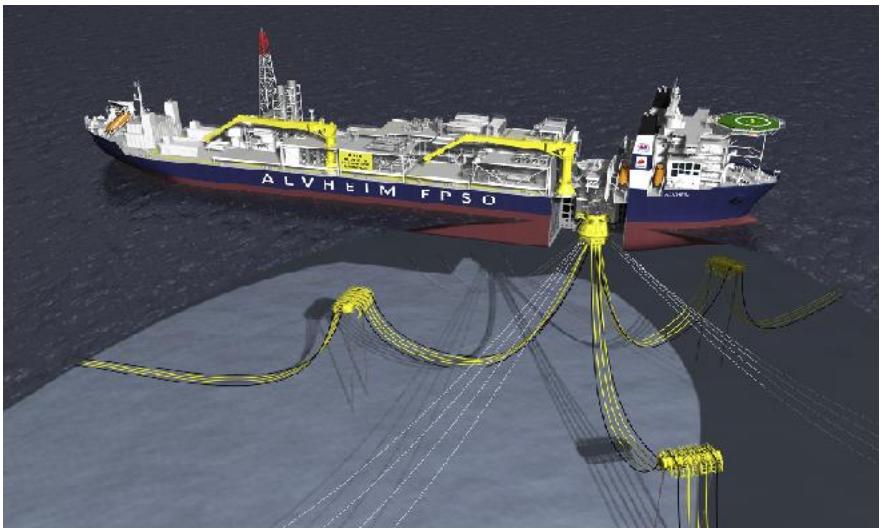

Figure 3-4 An ideal single-point mooring [3]

3.3 Mooring Line Components

For mooring purposes, the critical parameters for selecting a particular material are the breaking strength, elastic modulus, and submerged weight per unit length. It must be emphasised that the required breaking strength of a specific mooring configuration is dependent on the elastic modulus and submerged weight [18]. The mooring line can be a chain, fibre rope, wire rope, or a combination of the three. Thus, this segment discusses the main components of the mooring lines.

3.3.1 Chain

Chain is the most popular mooring component for station keeping in the offshore industry. It has two primary constructions, studlink and studless chains, as shown in Figure 3-5. Studlink chain is traditionally used for anchoring MODUs and FPSOs in relatively shallow water. It is proven and

tested as strong and reliable [19]. The use of studs avoids kinking and eases the handling of the chains. In addition, the studs can take some bending loads and help prevent deformation. However, these studs become loose during use and are often the initiation point for fatigue cracking [18].

Consequently, studless chains have been developed to fathom these problems. In addition, the end diameters of the studless chain have been reduced to decrease the bending loads. These chains are predominantly used for long-term moorings as fatigue damage is reduced due to the absence of studs [18].

The weight and stiffness properties of the chain, which are essential for the mooring analysis, are independent of grade. However, it must be emphasised that the stiffness and submerged weight of the studlink chain is approximately 10% more than the studless of the same diameter.

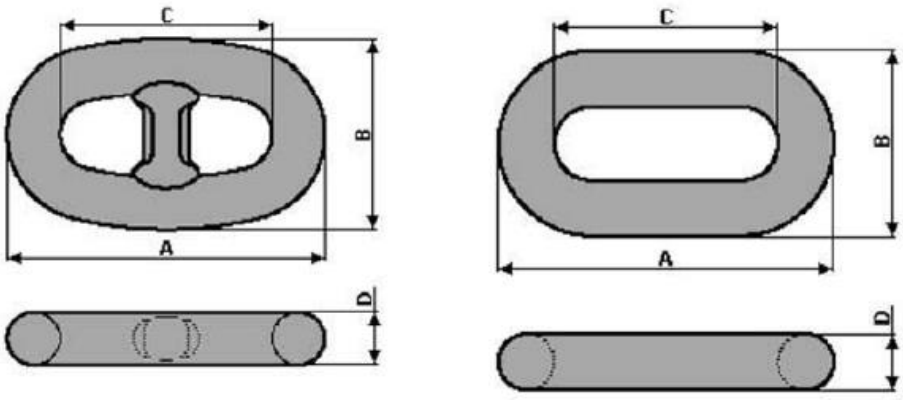

Figure 3-5 The studlink (left) and studless (right) chains [19]

Chain is available in various diameters and grades. Thus, Table 3-1 shows the varieties of chain grades concerning their mechanical properties, while Table 3-2 indicates the formula for calculating the proof and breaking test loads of the different chains.

Steel Grade	Yield Stress, R_e MPa	Tensile Strength, R_m MPa	Elongation, A_5 %	Area Reduction, Z %
R3	410	690	17	50
R3S	490	770	15	50
R4	580	860	12	50
R4S	700	960	12	50
R5	760	1000	12	50
R6	900	1100	12	50

Table 3-1 The minimum mechanical properties of the chain [20]

Grade	Proof Load (kN)		Breaking Load (kN)
	Studlink	Studless	
R3	$0.0156d^2(44-0.08d)$	$0.0156d^2(44-0.08d)$	$0.0223d^2(44-0.08d)$
R3S	$0.0180d^2(44-0.08d)$	$0.0174d^2(44-0.08d)$	$0.0249d^2(44-0.08d)$
R4	$0.0216d^2(44-0.08d)$	$0.0192d^2(44-0.08d)$	$0.0274d^2(44-0.08d)$
R4S	$0.0240d^2(44-0.08d)$	$0.0213d^2(44-0.08d)$	$0.0304d^2(44-0.08d)$
R5	$0.0251d^2(44-0.08d)$	$0.0223d^2(44-0.08d)$	$0.0320d^2(44-0.08d)$
R6	$0.0276d^2(44-0.08d)$	$0.0246d^2(44-0.08d)$	$0.0352d^2(44-0.08d)$
d = nominal diameter of the chain			

Table 3-2 The proof and breaking test loads formula [20]

3.3.2 Wire Rope

The wire rope has higher elasticity and is lighter in weight for the same breaking load than the chain [21]. It comprises various strands of metal wire twisted into a helix to form a strand. The pitch of the helix is fundamental in determining the flexibility and axial stiffness of the strand [19]. Figure 3-6 illustrates the typical wire rope constructions used for mooring applications.

According to Brown [19], the multi-strand rope is commonly used for MODUs and other temporary moorings as it is easy to handle. It may contain fibre or a metallic core to support the outer wires. The metallic core has an independent wire rope core (IWRC) and wire-strand core (WSC). IWRC is used more often for heavy marine applications.

Six-strand rope with IWRC is the most popular type used offshore for mobile drilling units as it has good lateral flexibility and is relatively cheap. However, the spiral strand is predominantly utilised for floating production systems due to its suitability for long-term installation. In addition, it provides greater longitudinal stiffness, torque balance, and lower spinning loss [18]. Brown [19] also noted that the spiral strand has more fatigue resistance than the multi-strand rope. DNVGL-OS-E304 [22] also states that it can be sheathed, preferably with polyethylene. The sheathing can also be provided with an axial stripe to control the possible twisting of the wire rope. In addition to the sheathing, zinc filler wire provides more corrosion resistance as it blocks the inside spaces between the wires to prevent saltwater entry [8]. API RP 2SK [8] reveals the life expectancy of the different types of wire ropes given in Table 3-3.

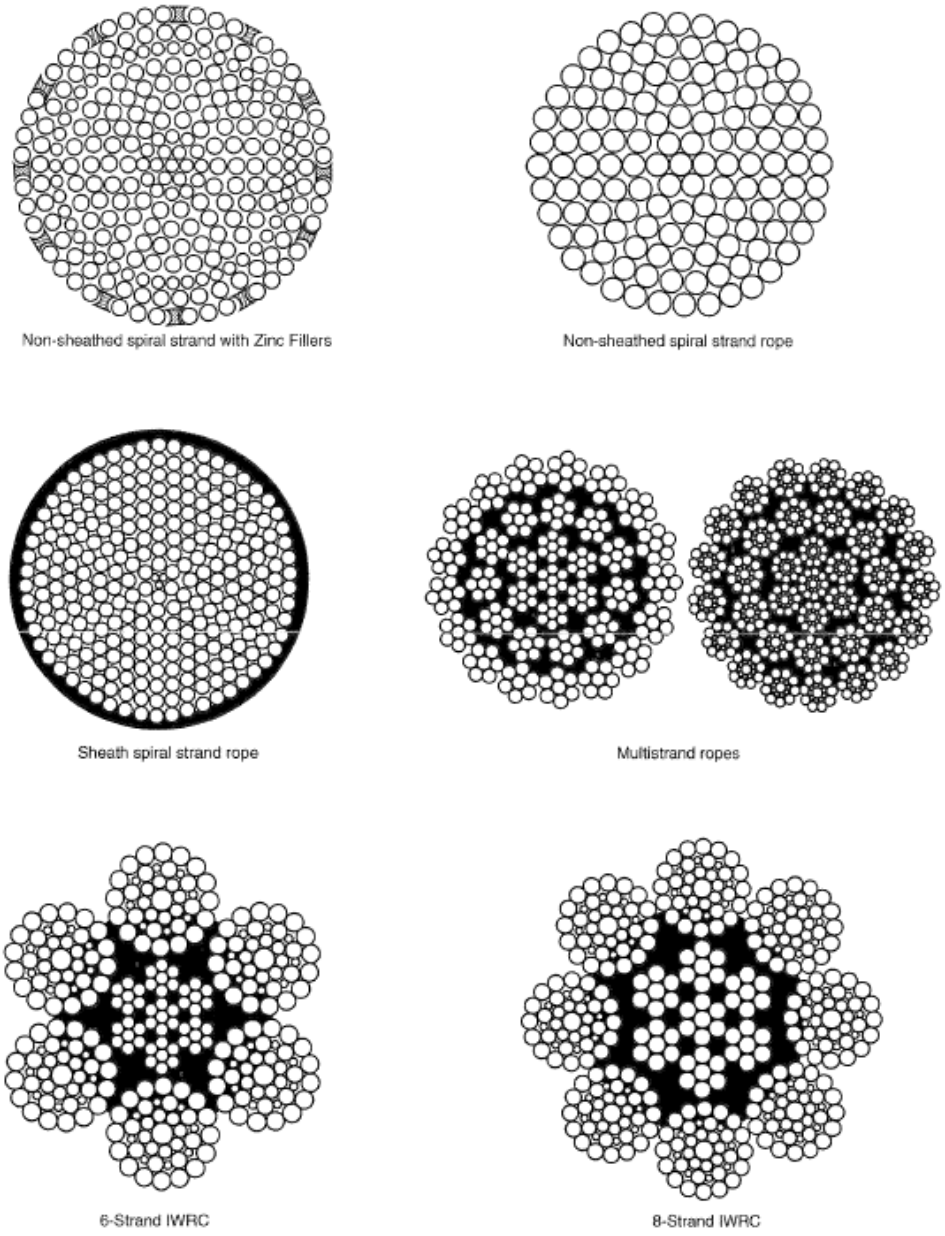

Figure 3-6 The typical wire rope constructions [8]

Type (Galvanized)	Life Expectancy (years)
Six-strand	6 – 8
Unjacketed spiral strand	10 – 12
Unjacketed spiral strand with zinc filler wires	15 – 17
Jacketed spiral strand	20 – 25
Jacketed spiral strand with zinc filler wires	30 – 35

Table 3-3 The life expectancy of the different types of wire ropes [8]

3.3.3 Fibre Rope

Generally, fibre rope is dominant over the other mooring line components in lightweight and elasticity [21]. Different types of fibre rope are considerably used for both temporary and permanent deepwater moorings. These are polyester (polyethylene terephthalate), aramid (aromatic polyamide), HMPE (high modulus polyethylene), and nylon (polyamide). Polyester is the best material for deepwater mooring applications regarding cost, dynamic tension, fatigue properties, resistance to axial compression fatigue, strength to weight ratio, and creep resistance. It is also the only fibre rope that has been placed in permanent moorings. Thus, HMPE and aramid are best for smaller rope diameters and ultra-deepwater mooring applications [8].

API RP 2SM [23] noted that nylon rope is used chiefly for hawsers in CALM systems. However, it is also used in shallow water applications where a length of nylon rope is inserted in the mooring line to soak up the energy from the vessel dynamics. Moreover, it is initially the most robust mooring rope among the four materials due to its high elasticity. Even so, it loses up to 15% strength when thoroughly wet. Therefore, it must be inspected frequently and replaced when needed.

Furthermore, jacketing plays a vital role in fibre rope constructions. It protects against soil ingress, marine growth, and fish bite. It is also utilised when external abrasion is likely to occur during installation and service. Thus, other factors affecting fibre ropes' life for deepwater mooring applications must be checked consistently, such as hydrolysis, heating and internal abrasion, tension-tension fatigue, axial compressive fatigue, and creep-rupture [8].

3.3.4 Connecting Link

Connecting link connects the main mooring line components. Some of its various types are shackles, swivels, wire clamps, and Kenter-type connecting links, as illustrated in Figure 3-7. According to Vryhof [21], shackles are the most common offshore connectors. It can be used whether in temporary or permanent moorings. However, the swivels are utilised in a temporary mooring system to reduce the twist and torque accumulated in the mooring line and are often placed near the anchor point.

On the other hand, the wire clamps are adjustable to fit the respective diameters of the wire rope. Vryhof [21] suggests that as the wire clamps add buoyancy bodies to a wire rope, the loads must be spread over the length of the wire to prevent bending damage. Finally, the Kenter type is mainly used to connect two pieces of a chain mooring line, provided both pieces have the exact dimensions. This connecting link has a shorter fatigue life than the chain, so it is not advisable to be used in permanent mooring systems.

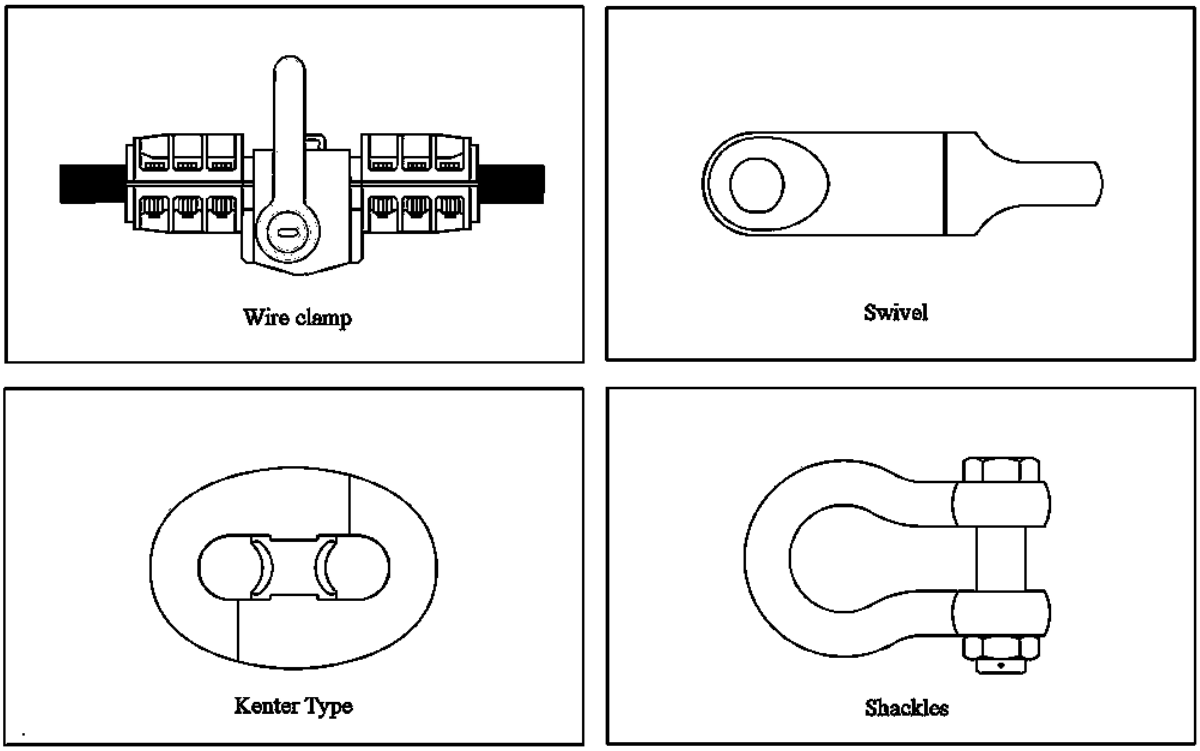

Figure 3-7 The connecting link types [21]

3.3.5 Anchoring Point

The anchor is attached to the end part of the mooring line that moors the vessel to the sea bottom. Vryhof [21] emphasises that the water depth, soil conditions, loads, and installation must be considered when selecting the anchor type. Figure 3-8 shows the typical anchoring points arranged by water depth and soil type. From left to right of the figure, the water depth is enumerated from shallow to ultradeep, while the soil condition is from hard to soft type.

The drag embedment is the most popular anchor type used until the present. It is designed to either partially or fully penetrate the seabed. The holding capacity is derived from the resistance of the

soil in front of the anchor. Dead weight is the oldest anchor that still exists today and is made of steel and concrete. Its holding capacity depends on the material's weight and the friction between the seabed and the anchor [21].

The driven pile and suction pile are hollow steel pipes in which the holding capacity is produced by combining the soil's friction and the anchor and lateral soil resistance. The driven pile is installed at a significant depth through driving hammers or a vibrator. On the other hand, the suction pile is placed by a pump attached to the top of the pipe. Additionally, both anchors can withstand horizontal and vertical loads [21].

Further, a gravity anchor positions itself without external energy and mechanical handling due to its drop weight. Thus, suitable for ultradeep water moorings. The vertical load anchor is positioned similarly to the drag embedment anchor but penetrates deeper [21].

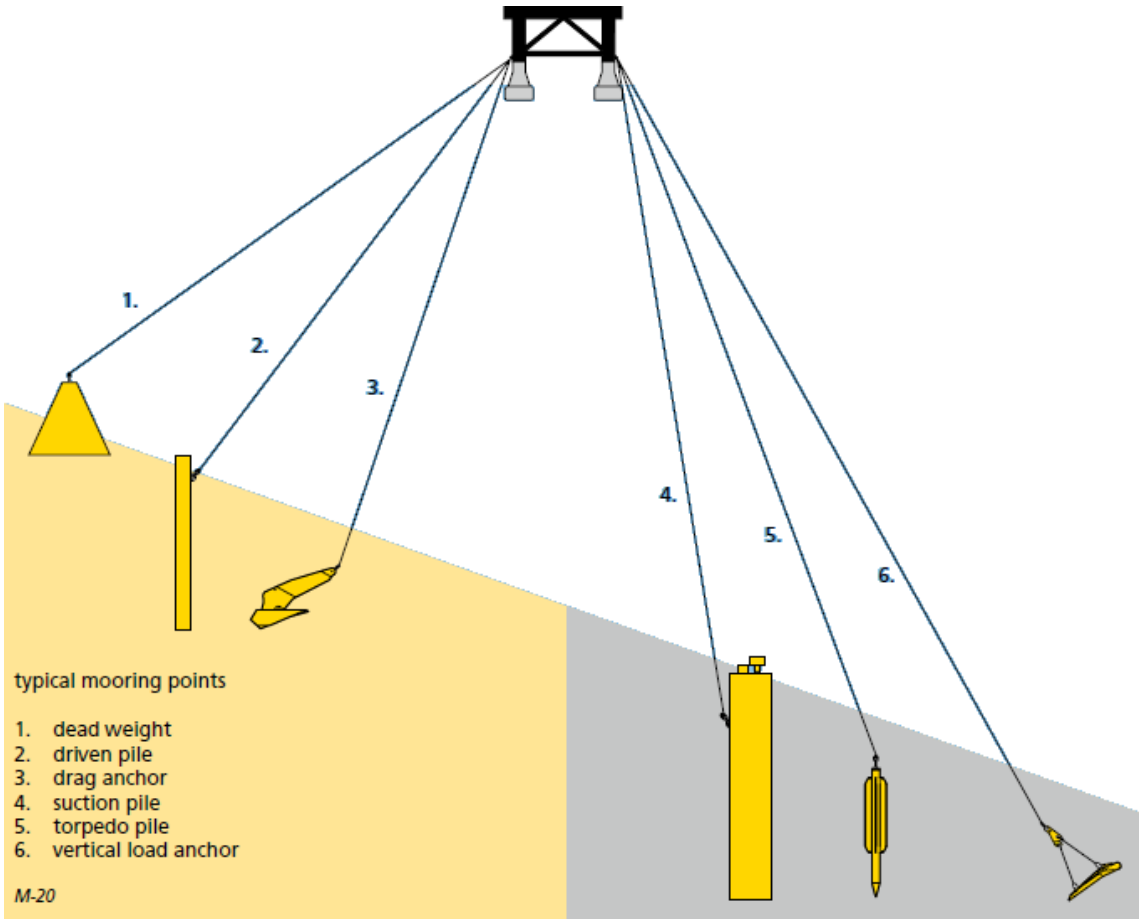

Figure 3-8 The typical anchoring points [21]

Chapter 4 Offshore Riser Systems

Risers are a critical subsea system for drilling, producing, and transporting hydrocarbons and other fluids related to oil and gas production. The risers link the floating structures to the oil and gas wells, subsea satellite wells, and export facilities [18]. These are mainly composed of conduit, interface with floater and wellhead, components, and auxiliary. Moreover, the risers must be arranged concerning stress and sectional forces, vortex-induced vibrations (VIV) and suppression, wave fatigue, and interference to keep external loading within permissible limits. Regarding material and installation costs, the risers must have sufficient flexibility allowing large excursions of the floating platform. Figure 4-1 presents an example of a drilling riser. Furthermore, this chapter discusses the two classifications of risers, rigid and flexible, in which the combination of the two is called a hybrid riser [24].

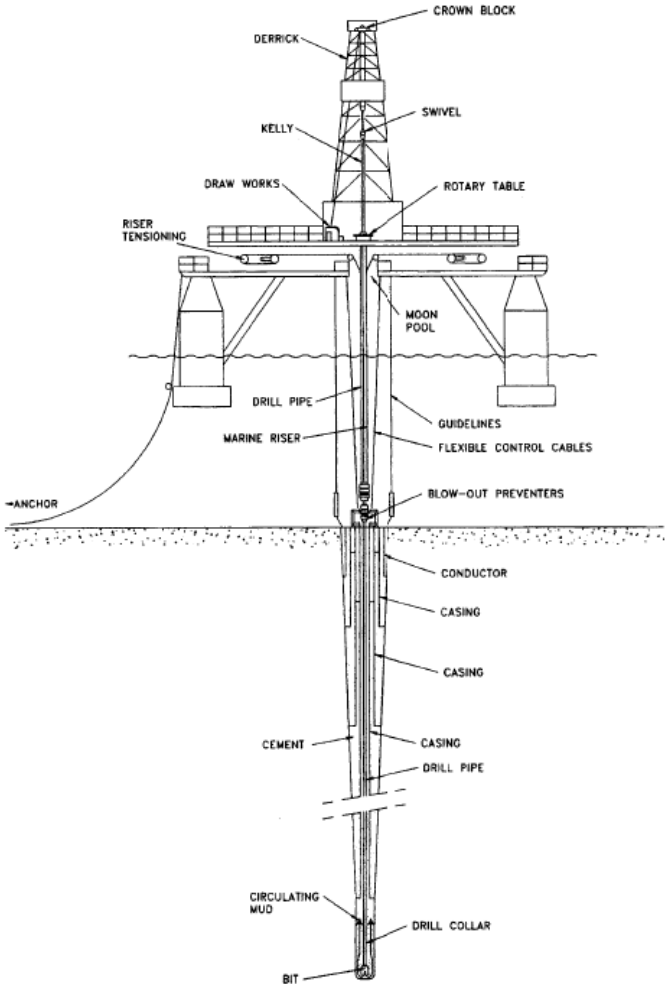

Figure 4-1 An illustrative sketch of a drilling riser [18]

4.1 Rigid Risers

A rigid riser, also known as a top tensioned riser (TTR), is vertical and usually manufactured from steel pipe. It is customarily tensioned to avoid buckling under its own weight, current and vortex shedding loads, and excessive bending stresses under a lateral wave. This type of riser is ideal when a large heavy workover is necessary. It is also an alternative when a polymer type of flexible riser cannot withstand the temperature or pressure of the fluids [18]. In addition, TTR uses a heave compensation system to allow the relative riser and floater motions in a vertical direction [25]. Drubers [26] also emphasises that TTR is only suitable for TLPs and spars having minimal lateral movement. Figure 4-2 shows illustrative sketches of a typical TTR.

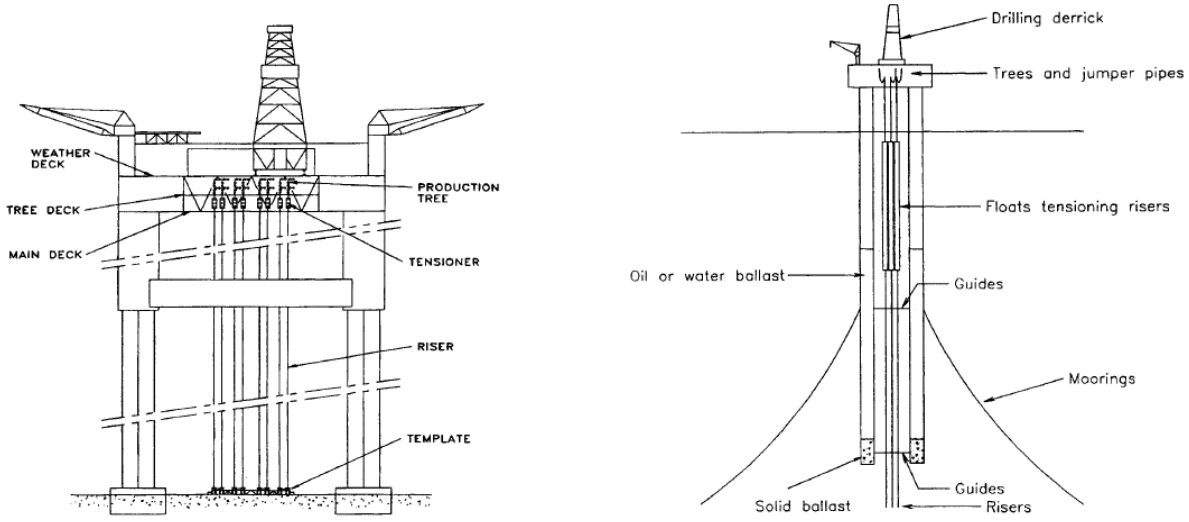

Figure 4-2 A TLP riser system (left) and a spar production platform (right) [18]

4.2 Flexible Risers

In contrast, flexible riser does not use heave compensation systems. Instead, it absorbs the motions of the floating structure by changing its geometry [25]. Flexible risers hang in catenaries. Thus, sufficient axial strength is needed to sustain catenary action. These kinds of risers are manufactured differently based on the depth of the water. In moderate water, layers of wires and polymers provide strength and allow the fluids to flow while the pipe is bent. Steel or titanium is used in deeper water, providing sufficient flexibility [18]. Bai and Bai [24] state that flexible risers can be installed in different configurations considering global behaviour and geometry, structural integrity, rigidity, continuity, cross-sectional properties, material, and costs. The static analysis

must determine which of the six main configurations is suitable for specific production and environmental requirement, as shown in Figure 4-3.

The CMPT [18] explains that the terms “lazy”, “steep”, and “pliant” refer to how the riser approaches the seabed. A lazy configuration is negatively buoyant near the seabed and lazily sets itself down or picks itself up as the tension changes. The buoyancy distribution approaches a termination on the seabed vertically in a steep configuration. The pliant configuration is like the lazy one. The only difference is that it is attached to a base by a tie as it approaches the seabed. The tie partially restricts movement while still permitting pliability as the tension varies.

Additionally, the wave configuration is supported by distributed buoyancy along their length to form a wavy curve in mid-water. As the S configuration is heavy, it may be anchored to the seabed by the riser or a separate tie [18]. Bai and Bai [24] also mention that the S configuration is only used if catenary and wave configurations are not suitable for a particular field as it requires complex installation.

Furthermore, the free-hanging catenary is the simplest and cheapest configuration yet subjected to extreme loading due to vessel motions that may cause compression buckling at the riser touch-down point. In addition, lazy waves are preferred to steep waves as they require minimal subsea infrastructure and can maintain their configuration while the riser fluid density changes [24].

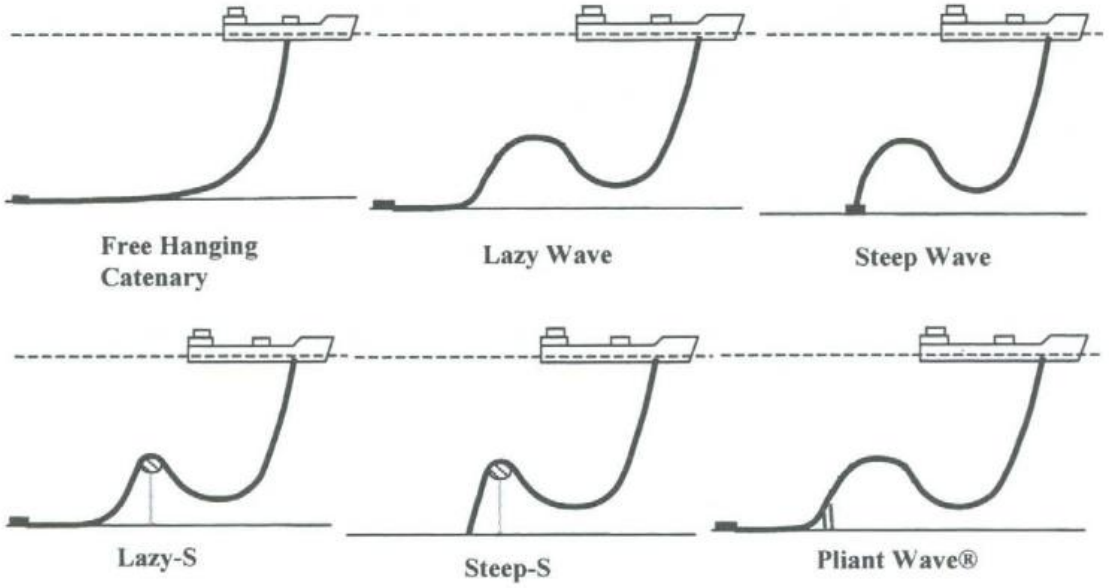

Figure 4-3 The main configurations of flexible risers [24]

4.3 Hybrid Risers

A hybrid riser combines rigid and flexible risers efficiently. It is used as production, export, import, and injection risers. Its typical configuration is a vertical or free-hanging riser from a submerged buoy to the seabed with a flexible riser from the buoy to the FPS [25]. Moreover, a combination of flexible jumpers, a vertical bundle of a rigid riser, and subsurface buoyancy is a proven concept for deepwater development [27].

A typical hybrid riser is illustrated in Figure 4-4. A flexible riser is connected to the floating structure, allowing a relative amount of motion between the two. Then, the flexible riser is attached to a buoyancy tank located 30 to 50 meters below the water surface. This buoyancy tank functions as a distribution station or connector called goosenecks. Finally, the tank is fastened to the rigid metal TTR anchored to the seafloor [26].

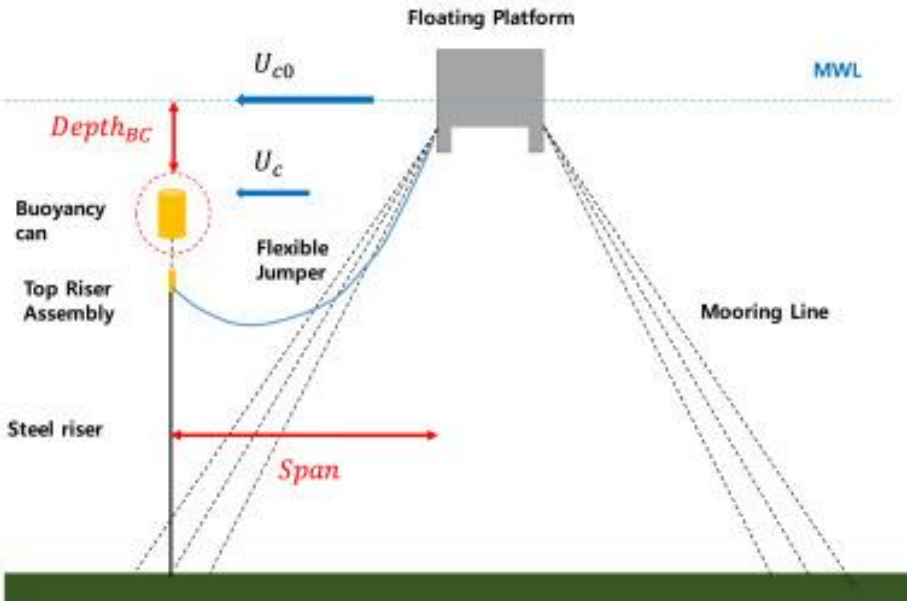

Figure 4-4 A representation of a hybrid riser [27]

Chapter 5 Environmental Loads and Fatigue Analysis

The typical approaches used to measure fatigue damage and fatigue life of the mooring system and the critical environmental loads and conditions to consider when designing the mooring systems are discussed in this chapter.

5.1 Fatigue Analysis

Fatigue refers to the progressive, localised, and permanent structural change in materials subjected to fluctuating stresses that may result in cracks or fractures after enough fluctuations. The main parameters influencing fatigue are stress difference, structural detail, material characteristics, and environmental factors. Fatigue is one of the primary reasons structural components fail [28]. Therefore, it needs to be appropriately considered when designing to avoid sudden failure of the structures during service.

5.1.1 S-N Approach

The S-N approach uses S-N curves which define the number of cycles to failure when a material is cycled repeatedly through a given stress range [29]. Equation 5.1 refers to the component capacity against tension fatigue [14]. Table 5-1 presents the fatigue parameters, while Figure 5-1 illustrates the S-N curves.

$$log[n_c(s)] = log(a_D) - m\,log(s) \tag{5.1}$$

where

$n_c(s)$ = number of cycles,

s = stress range (double amplitude),

a_D = intercept parameter of the S-N curve, and

m = slope of the S-N curve.

Component	a_D	m
Stud chain	$1.2 \cdot 10^{11}$	3.0
Studless chain (open link)	$6.0 \cdot 10^{10}$	3.0
Stranded rope	$3.4 \cdot 10^{14}$	4.0
Spiral rope	$1.7 \cdot 10^{17}$	4.8

Table 5-1 The S-N fatigue curve parameters [14]

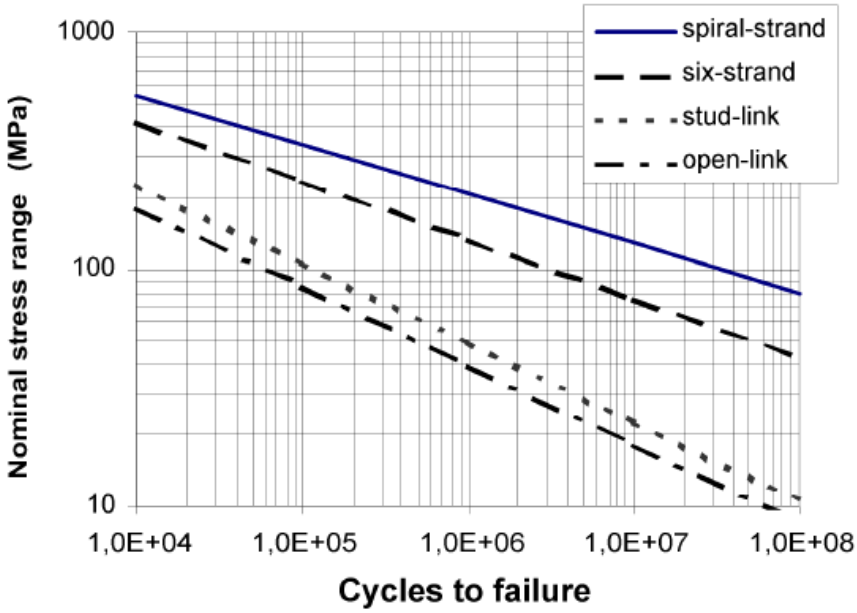

Figure 5-1 The mooring fatigue design S-N curves [14]

5.1.2 T-N Approach

The fatigue damage is calculated from the T-N curve related to the tension range rather than the stress range [29]. The T-N curve is presented by Equation 5.2 [8].

$$NR^M = K \tag{5.2}$$

where

N = number of cycles,

R = ratio of tension range (double amplitude) to MBS,

M = slope, and

K = intercept parameter.

Table 5-2 shows the *M* and *K* values. L_m is the ratio of mean load to reference breaking strength (RBS). The mean load is 30% of the minimum breaking strength (MBS). For chains and wire ropes, RBS is the same as MBS.

Component	m	K
Common studlink*	3.0	1000
Common studless link*	3.0	316
Six/multi-strand wire rope*	4.09	$10^{(3.20-2.79L_m)}$
Spiral strand wire rope*	5.05	$10^{(3.25-3.43L_m)}$
Polyester rope**	13.46	0.259

*** API RP 2SK [8]**
**** DNVGL-OS-E301 [14]**

Table 5-2 The M and K values

Furthermore, Figure 5-2 illustrates the fatigue design curves for different mooring components. It also reveals that the studless chain has shorter fatigue life than the studless chain. However, the latter has many fatigue issues related to studs. Thus, it is right to consider all fatigue life factors on selecting materials [8].

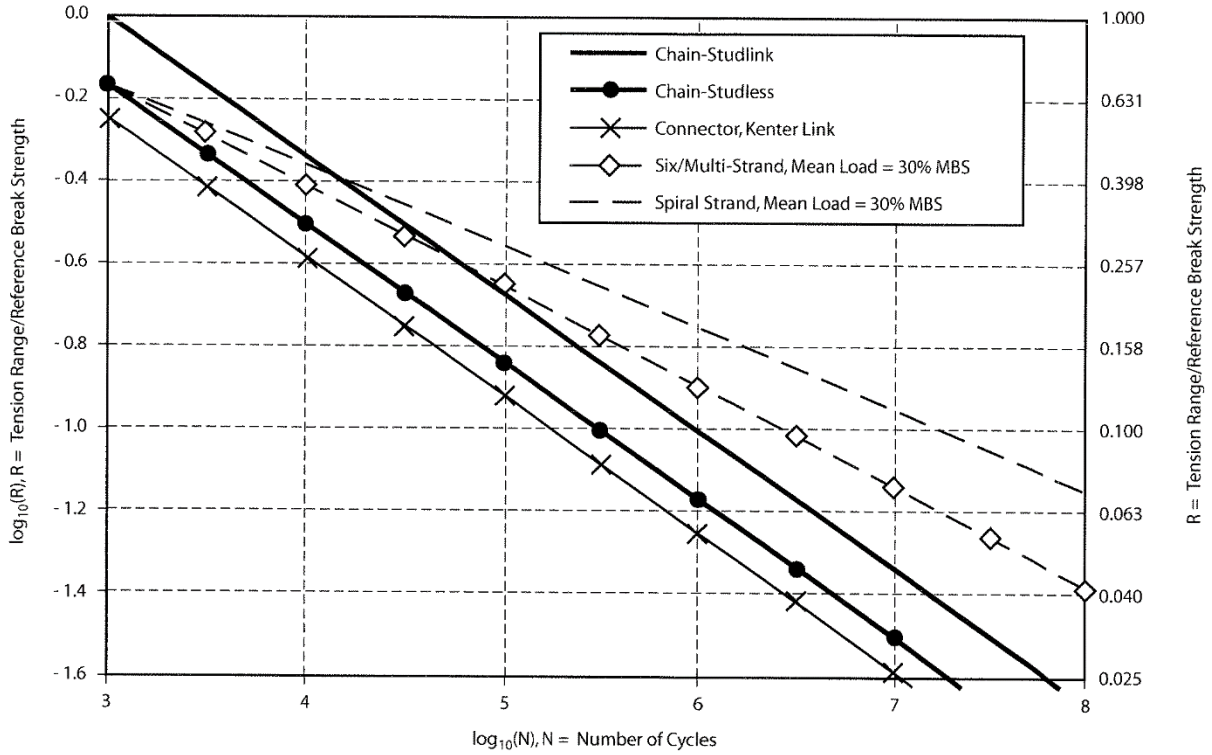

Figure 5-2 The mooring fatigue design T-N curves [8]

According to API RP 2SM [23], the fatigue test data for polyester ropes are available in the public domain and a design curve based on a regression analysis of 11 data points. On the other hand, the fatigue test data are limited for fibre ropes. Therefore, such data are inadequate to develop fatigue design curves for aramid, nylon, and HMPE. Table 5-3 indicates the polyester rope fatigue data.

Polyester Rope Data ($N_s = 11$)		
	Mean-1	Mean-2
$\boldsymbol{I}$	1.69	0.875
$\boldsymbol{K = 10I}$	48.8	7.50
$\boldsymbol{M}$	9.0	9.0

Table 5-3 The polyester rope fatigue data [23]

5.1.3 Miner's Rule

A mooring system's fatigue damage can be measured using S-N or T-N approaches. In addition, estimating the fatigue life is done by comparing the long-term cyclic loading and the resistance of a mooring component to fatigue damage. The Miner's Rule calculates the annual cumulative fatigue damage ratio [8]. However, Miner's rule does not account for the loading sequence effect, thus resulting in unreliable fatigue life predictions in variable amplitude loading conditions [28]. Equation 5.3 and Equation 5.4 calculate the fatigue damage and the fatigue life, respectively.

$$D = \sum_{i=1}^{n} \frac{n_i}{N_i} \tag{5.3}$$

$$L = \frac{1}{D} \tag{5.4}$$

where

D = annual cumulative fatigue damage ratio,

L = fatigue life,

n = number of load steps,

i = tension range interval,

n_i = number of cycles per year within the tension range interval, and

N_i = number of cycles to failure at normalised tension range as given by the appropriate T-N curve.

5.2 Environmental Loads and Conditions

API RP 2SK [8] mentions that the maximum design and operating conditions are the two classifications of environmental conditions that evaluate the strength of the mooring system. In maximum design conditions, the mooring system is intended to resist the extreme wind, waves, and current loads in a particular location. The environmental conditions usually represent a 100-year return period. However, API RP 2SK [8] suggests investigating the three sets of standards. These are the 100-year waves with associated winds and currents, the 100-year wind with associated waves and currents, and the 100-year current with associated waves and wind.

On the other hand, the maximum operating condition usually applies to the final design of the mooring system. This condition refers to the combination of wind, waves, and current in its maximum state and must not exceed the maximum design condition [8].

Environmental loads are categorised as steady loads, LF cyclic loads, and WF cyclic loads. The steady loads refer to the wind, current, and wave drift forces, which are constant in magnitude and direction for the duration of interest. On the other hand, LF cyclic loads excite the floating structures in a surge, sway, and yaw during natural periods. Furthermore, the periods of WF cyclic loads are usually from 5 to 30 seconds. This type of load is attained from WF responses, which are independent of mooring stiffness. However, WF motions can depend on the mooring stiffness if the natural period of the moored platform is close to the wave periods [8].

Though generally small compared to WF forces, LF forces are still accountable for the large excursion of the moored floating structures and the subsequent large load in the moorings. Note that the second-order wave forces become relatively large in severe storms. Therefore, it must be accounted for when designing the mooring system [30].

5.2.1 Wind

Typically, the wind has a stochastic nature that depends primarily on time and location. Therefore, API RP 2SK [8] recommends two methods to assess the effects of wind for design. First, the wind

is treated as constant in direction and speed, taking the one-minute average. Second, a steady component based on the 1-hour average velocity, combined with a time-varying component known as the gust. The latter, however, is used for the final design of permanent moorings. Also, DNV-RP-C205 [31] states that the 10-minute mean wind speed at 10 meters above the water surface with a 100-year return period should be used as a primary wind parameter.

Furthermore, as per DNVGL-OS-E301 [14], the Norwegian Petroleum Directorate (NPD) or the American Petroleum Institute (API) wind spectrum shall be applied to all locations. These wind spectrums are one-sided energy densities of the longitudinal wind speed fluctuations at a particular point. Therefore, when LF excitation is essential, the NPD wind spectrum must be utilised. It is worth noting that it has uncertainty for long periods, such as 500 seconds. Hence, the API upper bound spectrum can be used for more than 500 seconds [8].

5.2.1.1 NPD Wind Spectrum

The characteristic wind velocity may be determined using Equation 5.5. It is noteworthy that the averaging time must be less than $3600s$.

$$U(z,t) = U(z)\left[1 - 0.41 I_u(z)\, ln\left(\frac{t}{t_0}\right)\right] \tag{5.5}$$

where

$U(z,t)$ = characteristic wind velocity,
z = height above the water surface,
t = averaging time, and
t_0 = 3600 seconds.

The associated 1-hour mean wind speed and the turbulence intensity are calculated using Equation 5.6 and Equation 5.8, respectively.

$$U(z) = U_0\left[1 + C ln\left(\frac{z}{10}\right)\right] \tag{5.6}$$

$$C = 0.0573(1 + 0.15U_0)^{0.5} \tag{5.7}$$

$$I_u(z) = 0.06[1 + 0.043U_0]\left(\frac{z}{10}\right)^{-0.22} \tag{5.8}$$

where

$U(z)$ = 1-hour mean wind speed,

z = elevation above sea level,

U_0 = 1-hour mean wind speed at 10 meters above the water, and

$I_u(z)$ = turbulence intensity.

Moreover, the spectral energy density is defined by API RP 2SK [8] using Equation 5.9.

$$S_{NPD}(f) = \frac{320\left(\frac{U_0}{10}\right)^2\left(\frac{z}{10}\right)^{0.45}}{\left(1 + \tilde{f}^{0.468}\right)^{3.561}} \tag{5.9}$$

$$\tilde{f} = \frac{172f\left(\frac{z}{10}\right)^{\frac{2}{3}}}{\left(\frac{U_0}{10}\right)^{\frac{3}{4}}} \tag{5.10}$$

where

$S_{NPD}(f)$ = spectral energy density and

f = frequency.

5.2.1.2 API Wind Spectrum

According to API RP 2SK [8], Equation 5.11 determines the 1-hour mean wind speed, while Equation 5.13 calculates the wind gust speed.

$$U(z) = U_0\left(\frac{z}{z_R}\right)^{0.125} \tag{5.11}$$

$$z_R = 10m \tag{5.12}$$

$$U(z,t) = U(z)[1 + g(t)I(z)] \tag{5.13}$$

$$g(t) = 3 + ln\left(\frac{3}{t}\right)^{0.6} \tag{5.14}$$

where

$U(z)$ = 1-hour mean wind speed,

U_0 = 1-hour mean wind speed at 10 meters above sea level,

z = height above sea level,

z_R = reference elevation,

$U(z,t)$ = wind gust speed,

t = wind speed averaging time less than $60s$, and

$I(z)$ = turbulence intensity.

The turbulence intensity can be determined using the two equations. Equation 5.15 must be used when $z \leq 20$. Otherwise, use Equation 5.16.

$$I(z) = 0.15\left(\frac{z}{20}\right)^{-0.125} \tag{5.15}$$

$$I(z) = 0.15\left(\frac{z}{20}\right)^{-0.275} \tag{5.16}$$

Furthermore, API RP 2SK [8] computes the spectral energy density, $S_{API}(f)$, using Equation 5.17.

$$S_{API}(f) = \frac{\sigma(z)^2}{f_p\left(1 + 1.5\frac{f}{f_p}\right)^{\frac{5}{3}}} \tag{5.17}$$

$$\sigma(z) = I(z)U(z) \tag{5.18}$$

$$f_p = \frac{0.025\,U(z)}{z} \tag{5.19}$$

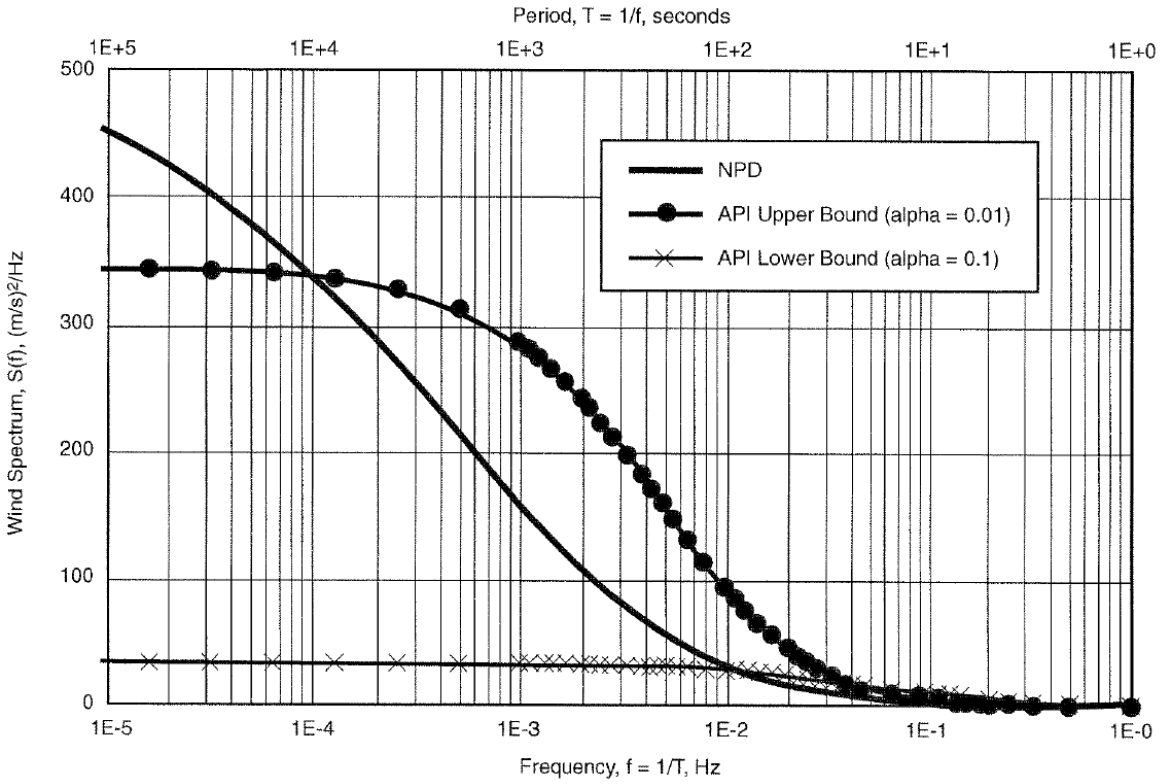

Figure 5-3 The 1-hour mean wind speed at 10 meters above sea level [8]

Figure 5-3 compares NPD and API wind spectrums for a 1-hour mean wind speed at 10 meters above sea level.

5.2.2 Wave

Applying wave spectra in deterministic design wave methods or stochastic methods determines the wave conditions. Deterministic regular waves characterised by wavelength, wave period, wave height, and crest height must be used for the quasi-static response of structures. On the other hand, a structure with significant dynamic response requires stochastic modelling of the sea surface and its kinematics by time series [31, 32].

In a sea state, the wind seas and swell are the two categories of wave conditions. The waves that moved out of the areas where they were generated and had no relationship to the local wind are called swells, while wind seas are generated by local wind [31, 32].

Furthermore, a design sea state is one in which a response's lifetime extreme value is expected to occur. The wave height and wave period relationships are essential for the design sea state. As a

result, these must be accurately determined from the desired location's oceanographic data. Various wave periods should be investigated as the period significantly affects the wave drift forces and vessel motions [8]. These data can be collected through in situ methods and remote sensing. In addition, sea states with return periods of 100 years shall be used [14].

DNVGL-RP-C205 [31] describes waves as irregular and random in shape, height, length, and propagation speed. Therefore, a wave spectrum may describe irregular sea states such as JONSWAP, Pierson-Moskowitz, and Ochi-Hubble.

5.2.2.1 Pierson-Moskowitz Spectrum

The Pierson-Moskowitz is a single peak, one-dimensional spectrum with no wave energy spreading. Therefore, the PM spectrum for a fully developed sea is given by Equation 5.20.

$$S_{PM}(\omega) = \frac{5}{16} \cdot {H^2}_s {\omega^4}_p \cdot \omega^{-5} exp\left[-\frac{5}{4}\left(\frac{\omega}{\omega_p}\right)^{-4}\right] \tag{5.20}$$

where

ω = wave frequency and

ω_p = spectral peak frequency.

5.2.2.2 JONSWAP Spectrum

The JONSWAP spectrum, as defined by Equation 5.21, is a modified version of the PM spectrum. Thus, it represents a developing sea state in a limited fetch situation.

$$S_J(\omega) = A_\gamma S_{PM}(\omega) \gamma^{exp\left[-0.5\left(\frac{\omega-\omega_p}{\sigma\omega_p}\right)^2\right]} \tag{5.21}$$

$$A_\gamma = 1 - 0.287 \ln \gamma \tag{5.22}$$

where

γ = non-dimensional peak shape parameter,

σ = spectral width parameter, and

σ_a for $\omega \leq \omega_p$

σ_b for $\omega > \omega_p$

A_γ = normalising factor.

The average values for the experimental data are $\gamma = 3.3$, $\sigma_a = 0.07$, and $\sigma_b = 0.09$. For $\gamma = 1$, JONSWAP wave spectrum reduces to the PM wave spectrum. Equation 5.23 shows a relationship that the JONSWAP spectrum must meet.

$$3.6 < \frac{T_p}{\sqrt{H_s}} < 5 \tag{5.23}$$

Figure 5-4 presents the effect of the peak shape parameter. However, if peak shape values are missing, the following equations may be used.

$$\frac{T_p}{\sqrt{H_s}} \leq 3.6, \qquad \gamma = 5 \tag{5.24}$$

$$3.6 < \frac{T_p}{\sqrt{H_s}} < 5, \qquad \gamma = exp\left(5.75 - 1.15\frac{T_p}{\sqrt{H_s}}\right) \tag{5.25}$$

$$5 \leq \frac{T_p}{\sqrt{H_s}}, \qquad \gamma = 1 \tag{5.26}$$

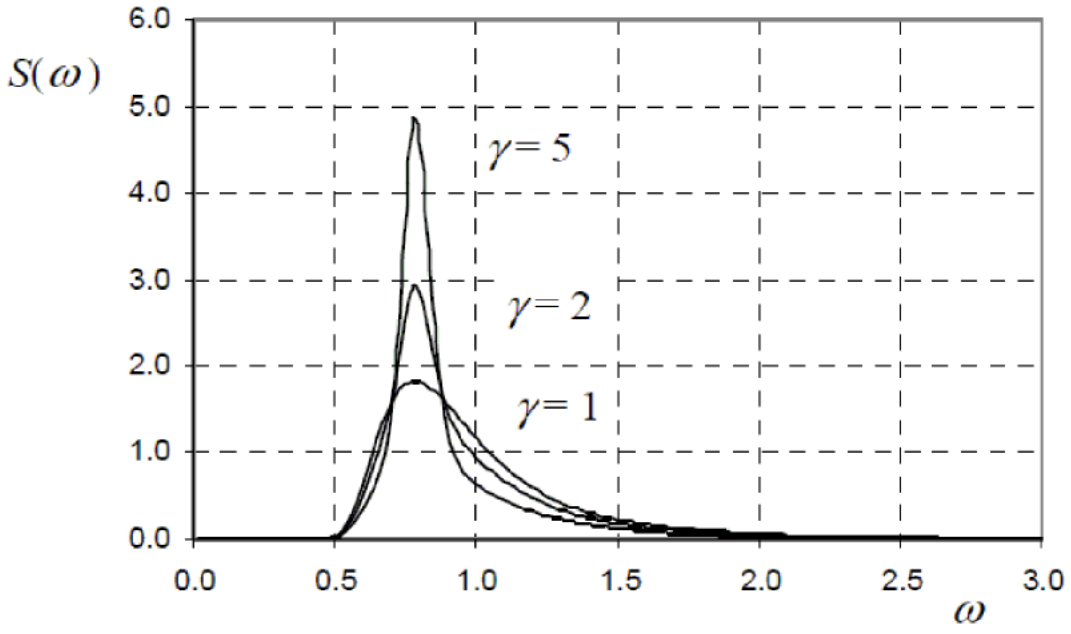

Figure 5-4 A JONSWAP wave spectrum for $H_s = 4\ m$ and $T_p = 8\ s$ [32]

5.2.2.3 Ochi-Hubble Spectrum

The combination of two different sea states describes the Ochi-Hubble spectrum. It is a sum of two Gamma distributions, each with significant wave height, spectral peak period, and shape factor for each wave system. The Ochi-Hubble spectrum is defined by Equation 5.27.

$$S(\omega) = \sum_{j=1}^{2} E_j G_j \Gamma_j \tag{5.27}$$

$$E_j = \frac{H^2{}_{s,j} T_{p,j}}{32\pi} \tag{5.28}$$

$$\Gamma_j = {\omega_{n,j}}^{-4(\lambda_j+0.25)} \cdot exp^{-(\lambda_j+0.25){\omega_{n,j}}^{-4}} \tag{5.29}$$

$$G_j = \frac{4(\lambda_j + 0.25)^{\lambda_j}}{\Gamma(\lambda_j)} \tag{5.30}$$

$$\omega_{n,j} = \frac{\omega T_{p,j}}{2\pi} \tag{5.31}$$

where

$H_{s,j}$ = significant wave height,

$T_{p,j}$ = spectral peak period, and

λ_s = shape factor.

For lower and higher frequency components, use $j = 1$ and $j = 2$, respectively. Moreover, the significant wave height for the sea state is given by Equation 5.32.

$$H_s = \sqrt{H^2{}_{s,1} + H^2{}_{s,2}} \tag{5.32}$$

5.2.3 Current

Typically, a surface current speed with a 10-year return period should be used for design. Currents have different effects on every offshore structure. It causes large steady excursions and slow drift motions to floating platforms, while it gives rise to drag and lift forces on submerged structures. It

also gives rise to VIV of slender structural elements and VIM of large volume structures. In addition, currents create seabed scouring all over the bottom-mounted structures. Therefore, these effects of currents must be considered in offshore structures design [31, 14].

Moreover, Equation 5.33 can be used if statistical data for open areas with wind-generated current velocities at the still water level is unavailable.

$$V_{c_{wind}} = 0.015U_{1hour,10m} \tag{5.33}$$

Chapter 6 Design of Mooring Systems: Considered Cases for Fatigue Analysis

A turret moored FPSO with nine mooring lines is utilised as a case study. This chapter presents the three cases of mooring systems used to select the best design for the given sea states. In addition, the metocean data taken from GOM, software used, specifications of FPSO, mooring system particulars, and fatigue parameters are also presented in this chapter.

6.1 Software

The software used in this study is OrcaFlex. It performs global static and dynamic analyses of the moorings. Subsequently, the fatigue analysis is carried out to calculate the fatigue damage and life of the mooring lines.

6.2 FPSO

The FPSO with an internal turret used as a case study is the default vessel in the OrcaFlex software since the centre of this thesis is the mooring system and not the vessel. The turret is modelled as a constraint object to manage the vessel's degrees of freedom. The water depth used is 400 meters. The dimensions and the particulars of FPSO are given in Table 6-1.

Figure 6-1 The FPSO with internal turret

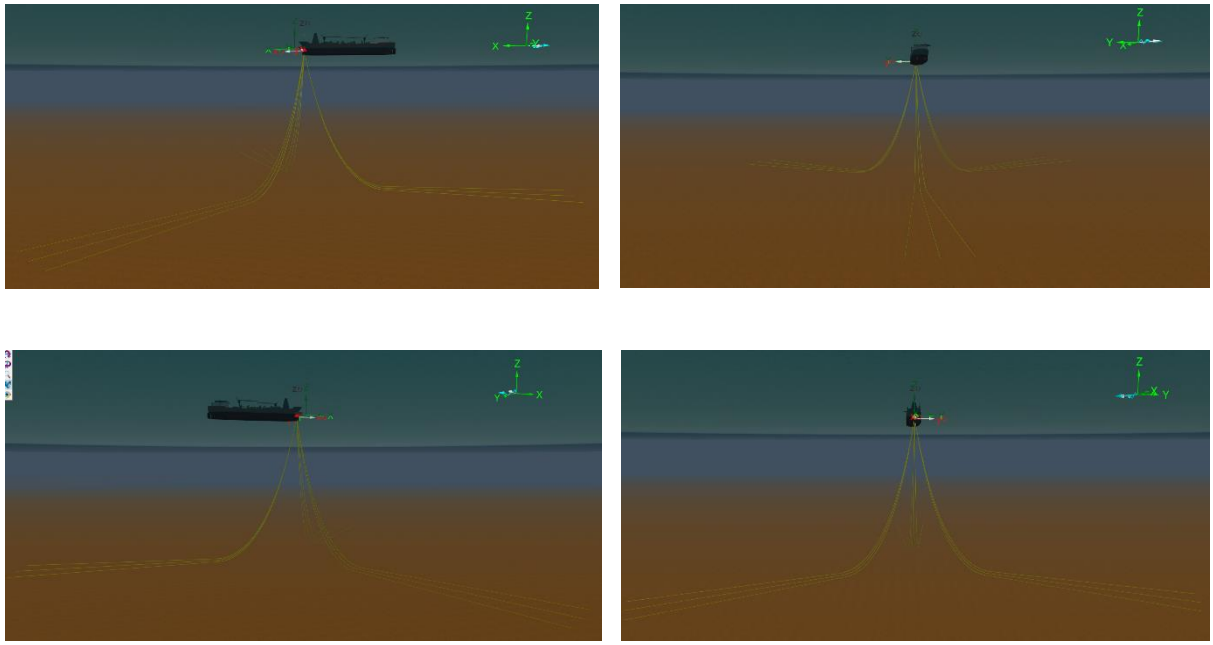

Figure 6-2 The FPSO with the mooring system

Parameters	Symbol	Unit	Quantity
Length Between Perpendiculars	LPP	m	103
Displacement	Δ	tonnes	8800
Breadth	B	m	15.95
Depth	H	m	13.32
Draft	D	m	6.66
Transverse Metacentric Height	GM_t	m	1.84
Longitudinal Metacentric Height	GM_l	m	114
Block Coefficient	C_b		0.804
Centre of Mass (x, y, z)	COG	m	2.53, 0, -1.974
Turret's Location (x, y, z)	Fairlead	m	33, 0, -6.66

Table 6-1 The FPSO's main particulars [29]

6.3 Mooring System

The catenary mooring configuration is applied. The mooring system consists of nine mooring lines divided into three clusters, as shown in Figure 6-3. Cluster 1 consists of lines 1 to 3, while cluster 2 comprises of lines 4 to 6, and cluster 3 includes lines 7 to 9. In this study, the design of the

mooring line is the same, as illustrated in Figure 6-4. The degree between the three lines is 5. In addition, all the cases have the same segment length to determine the best mooring system for the fatigue operational sea states in GOM. The different cases with their corresponding mooring systems and the properties of mooring lines are presented in Table 6-2 and Table 6-3, respectively.

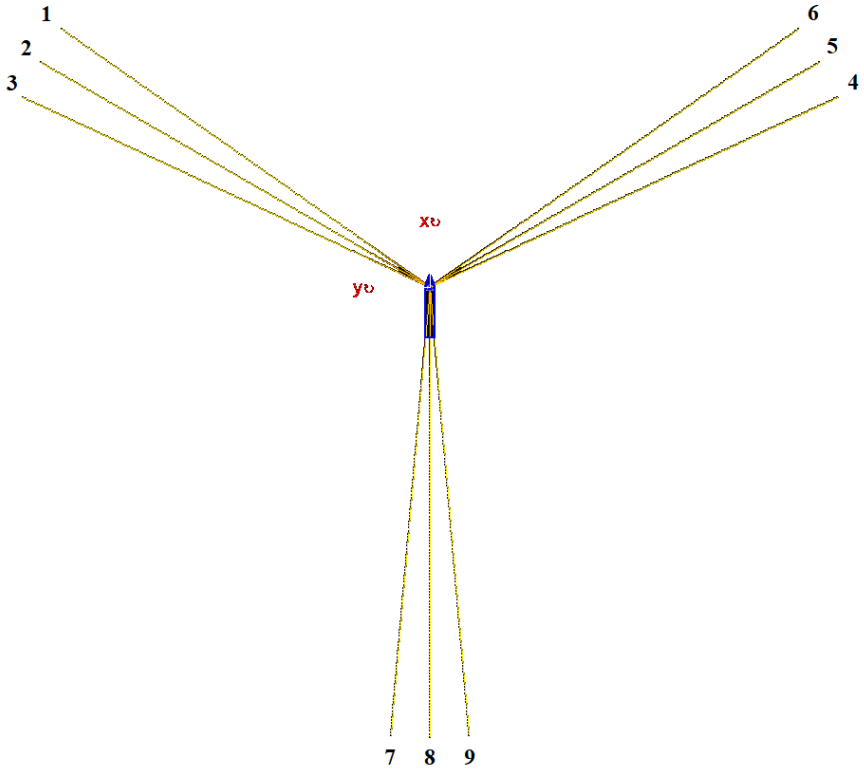

Figure 6-3 The mooring arrangement

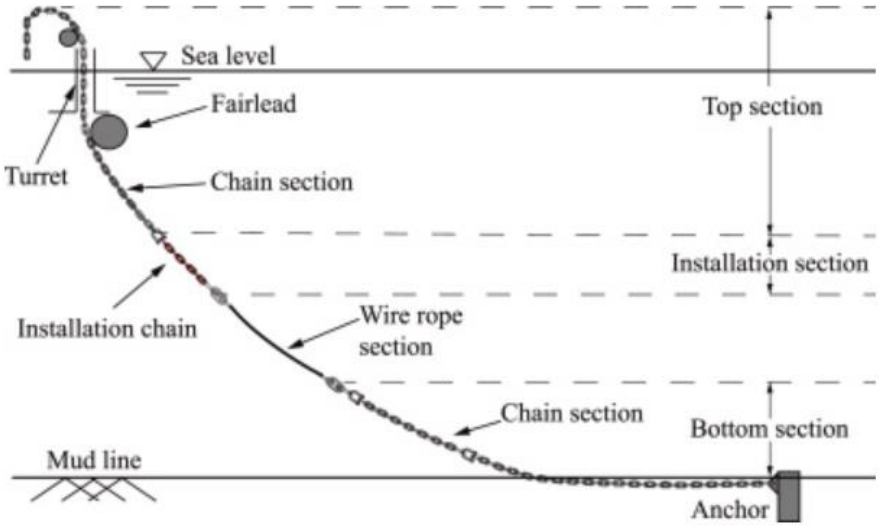

Figure 6-4 An illustration of a typical mooring line [33]

Cases	Mooring Systems
Case 1	chain-chain-chain
Case 2	chain-polyester rope-chain
Case 3	chain-wire rope-chain

Table 6-2 The different mooring systems used in case studies

Line Segment (Fairlead to Anchor)	Length (m)	Diameter (m)	Weight (kN/m)	Submerged Weight (kN/m)	Axial Stiffness (MN)	Mean Breaking Load (kN)
			Case 1			
Chain (R4, studless)	1000	0.089	1.5458	1.3432	676.50	8004.27
			Case 2			
Chain (R4, studless)	300	0.089	1.5458	1.3432	676.50	8004.27
Polyester (8-strand)	300	0.089	0.0620	0.0157	8.6339	1350.27
Chain (R4, studless)	400	0.089	1.5458	1.3432	676.50	8004.27
			Case 3			
Chain (R4, studless)	300	0.089	1.5458	1.3432	676.50	8004.27
Wire (6x19 with wire core)	300	0.089	0.3099	0.2699	320.00	5016.83
Chain (R4, studless)	400	0.089	1.5458	1.3432	676.50	8004.27

Table 6-3 The main properties of mooring lines

6.4 Metocean Conditions

The metocean parameters for permanent mooring systems must be well-defined. Also, it must be emphasised that FLS must consider a broader range of weather states. In contrast, ULS and ALS consider the same weather conditions. Table 6-4 presents the operational fatigue seastates in GOM with a frequency of occurrence in percentages. A non-collinear environment is utilised in this study, as presented in Table 6-5. The direction of the waves is 180 degrees, approaching the bow of the FPSO. The wind is 30 degrees relative to the waves, while the current is 45 degrees to the waves. Note that the wind and current act towards the same side of the FPSO.

Bin	Wave			Wind (m/s)	Current (m/s)	Total (%)
	H_s (m)	T_p (s)	γ			
1	0.5	5	1	11	0.2	28.542
2	0.5	7	1	11	0.2	20.714
3	0.5	10	1	11	0.2	4.707
4	1.1	13	1	11	0.2	0.192
5	1.5	5	1	11	0.2	17.562
6	1.5	9	1	11	0.2	17.299
7	2.5	11	1	11	0.2	1.051
8	2.7	6	1	11	0.2	9.313
9	3.5	11	1	11	0.2	0.144
10	4.7	6	1	13	0.2	0.352
11	5.1	9	2	15	0.2	0.034
12	8.3	6	2	21	0.3	0.089
Total						**100**

Table 6-4 The GOM operational fatigue seastates [1]

Environmental Conditions	Type	Direction (degrees)
Wave	JONSWAP	180
Wind	NPD Spectrum	210
Current		225

Table 6-5 The types and directions of environmental loads used in the case study

6.5 Fatigue Parameters

For this study, the T-N curves are employed in calculating the fatigue damage of the mooring lines against tension ranges. The total load case damage values for all load cases are summed up to determine the total damage using rainflow analysis. Table 6-6 indicates the parameters used for the fatigue analysis of the moorings.

Parameters	m	K	Breaking Strength (kN)
Chain (studless)	3.0	316	8004.27
Polyester rope	13.46	0.259	1350.27
Wire	4.09	230.67	5016.83

Table 6-6 The fatigue parameters of mooring lines

Chapter 7 Design of Mooring Systems: Results and Discussions

This section provides the numerical analysis results of the turret moored FPSO mooring system with the GOM metocean parameters. In addition, the fatigue damage caused by LF, WF, and the combined responses is analysed. This study focuses on the four fatigue locations along the mooring lines: the chain at fairlead, the chain at the bottom of the top chain, the chain at the top of the bottom chain, and the chain at the seabed interaction point. Finally, three case studies are conducted to determine the best mooring system for the parameters presented in Chapter 6. Note that a catenary mooring configuration is used in this study. The numerical results of the mooring system's fatigue life and damage are tabulated in Appendix A and Appendix B, respectively. Therefore, this chapter only shows the graphical representation of the results.

7.1 Case 1: chain-chain-chain system

Case 1 comprises an all-chain system, with each mooring line having a total length of 1000 meters. This system requires a high initial tension and is challenging to install in deeper locations. The longer the line, the more costly it becomes.

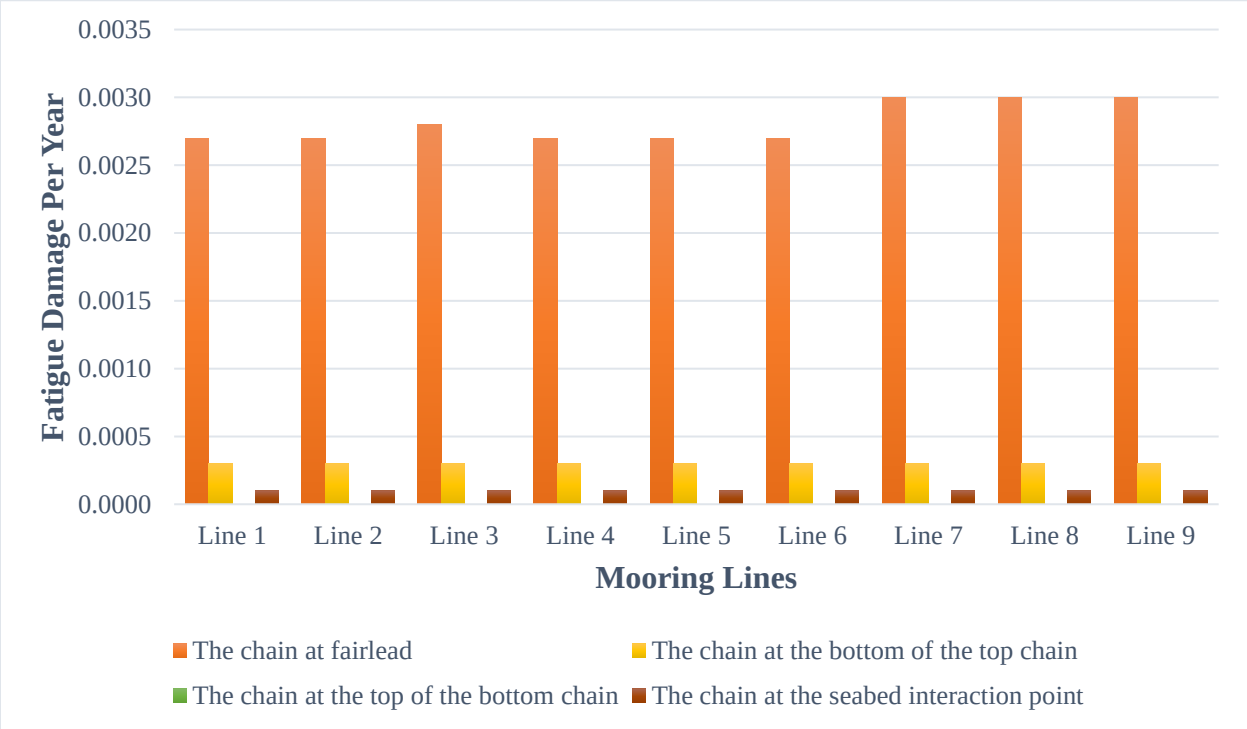

Figure 7-1 The fatigue damage considering an LF motion for case 1

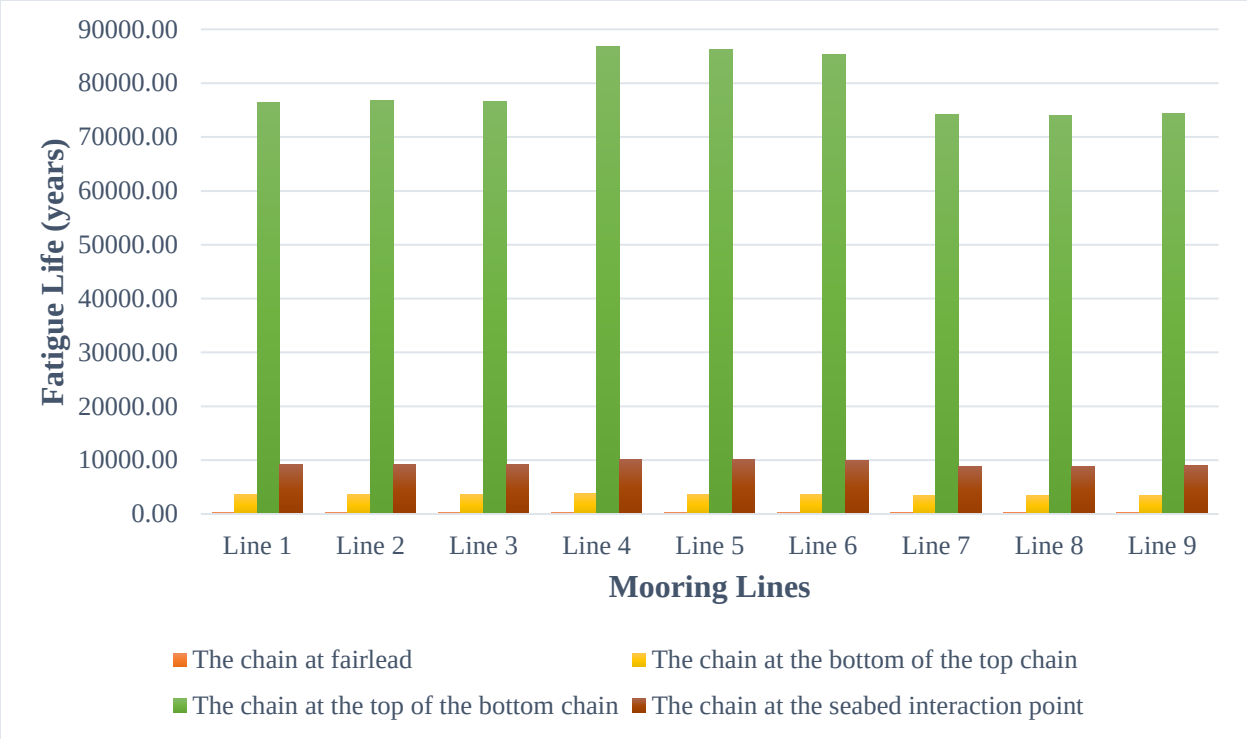

Figure 7-2 The fatigue life considering an LF motion for case 1

Figure 7-1 reveals that the critical fatigue damage induced by LF motion occurs at fairlead for all mooring lines. That is proven by Figure 7-2, which shows that the chain at the fairlead has the shortest fatigue life. Therefore, the most critical mooring are lines 7, 8, and 9, each having fatigue damage of 0.0030 per year. Line 3 has 0.0028, while lines 1, 2, 4, 5, and 6 have 0.0027 fatigue damage.

For all nine mooring lines, Figure 7-2 indicates that the chain at the top of the bottom chain has the highest fatigue life, followed by the chain at the seabed interaction point, then the chain at the bottom of the top chain, and finally the chain at the fairlead. Considering LF motion, the fatigue life of the chain-chain-chain mooring system is 331.79 years.

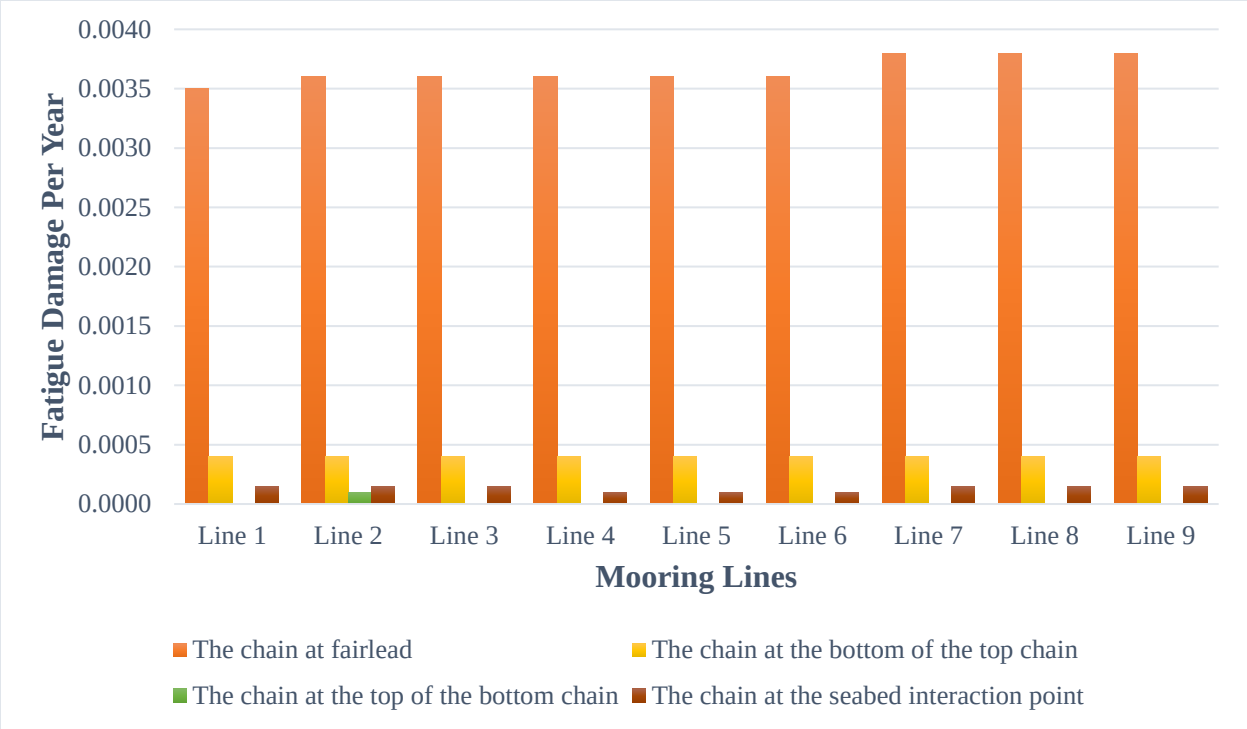

Figure 7-3 The fatigue damage considering a WF motion for case 1

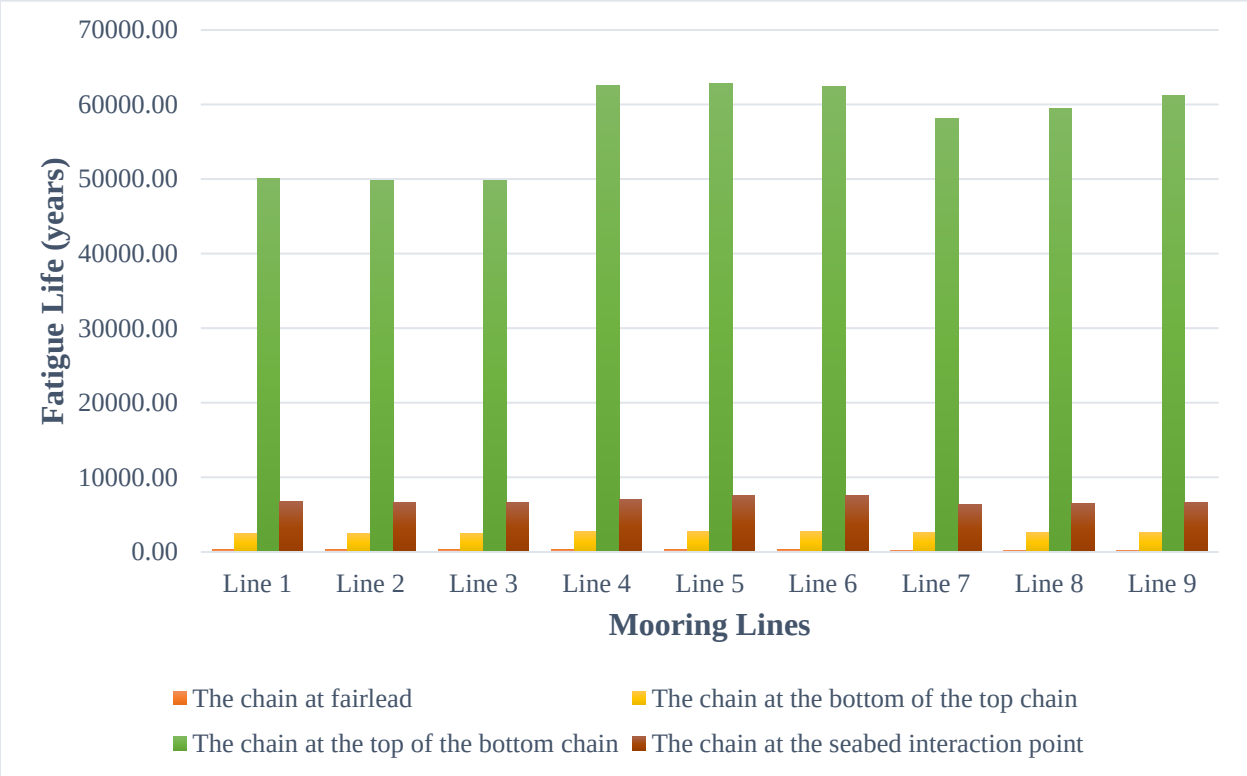

Figure 7-4 The fatigue life considering a WF motion for case 1

Similarly, as presented in Figure 7-3, the critical fatigue damage by WF motion happens at fairlead. That is due to the catenary configuration of the mooring lines that is susceptible to more significant viscous damping. Lines 7 to 9 have fatigue damage of 0.0038 per year. The fatigue damage of lines 2 to 6 is 0.0036, while line 1 has 0.0035. Hence, WF response generates more significant fatigue damage than LF response. As shown in Figure 7-4, line 9 is the most critical, having a fatigue life of 260.61 years. The result is approximately 21% lesser than LF motion.

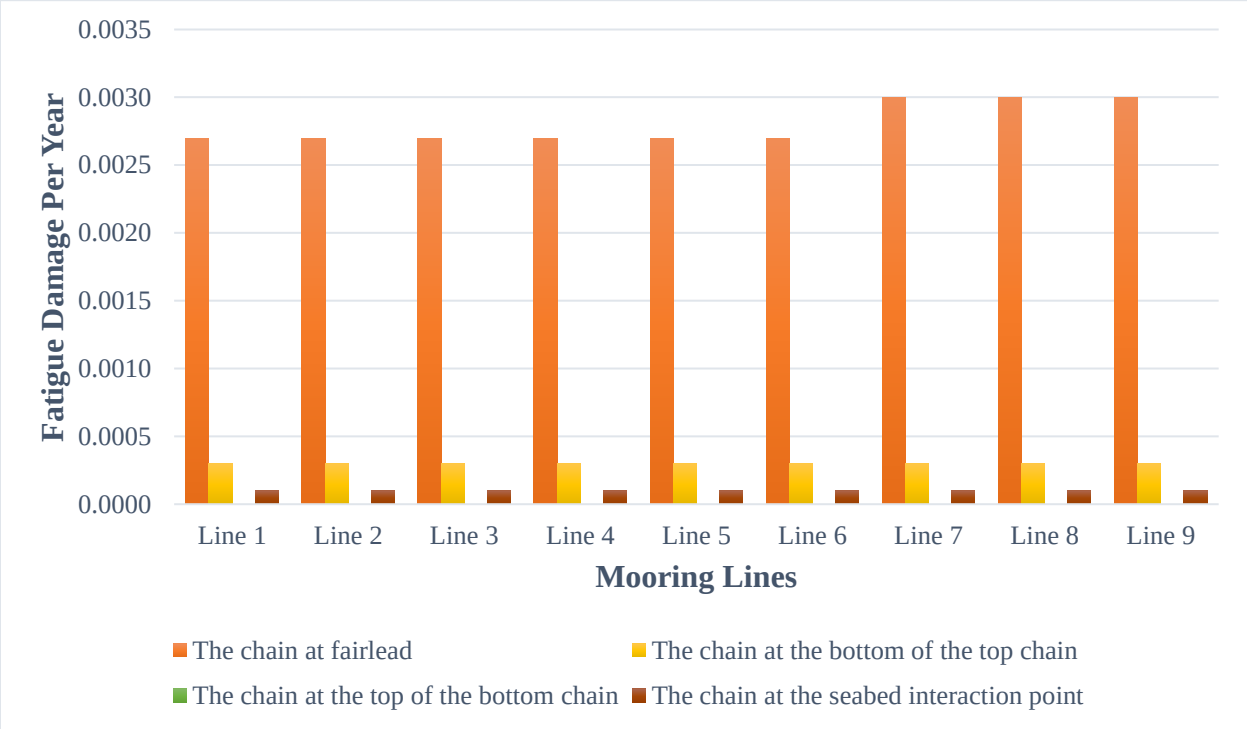

Figure 7-5 The fatigue damage considering the combined LF and WF motions for case 1

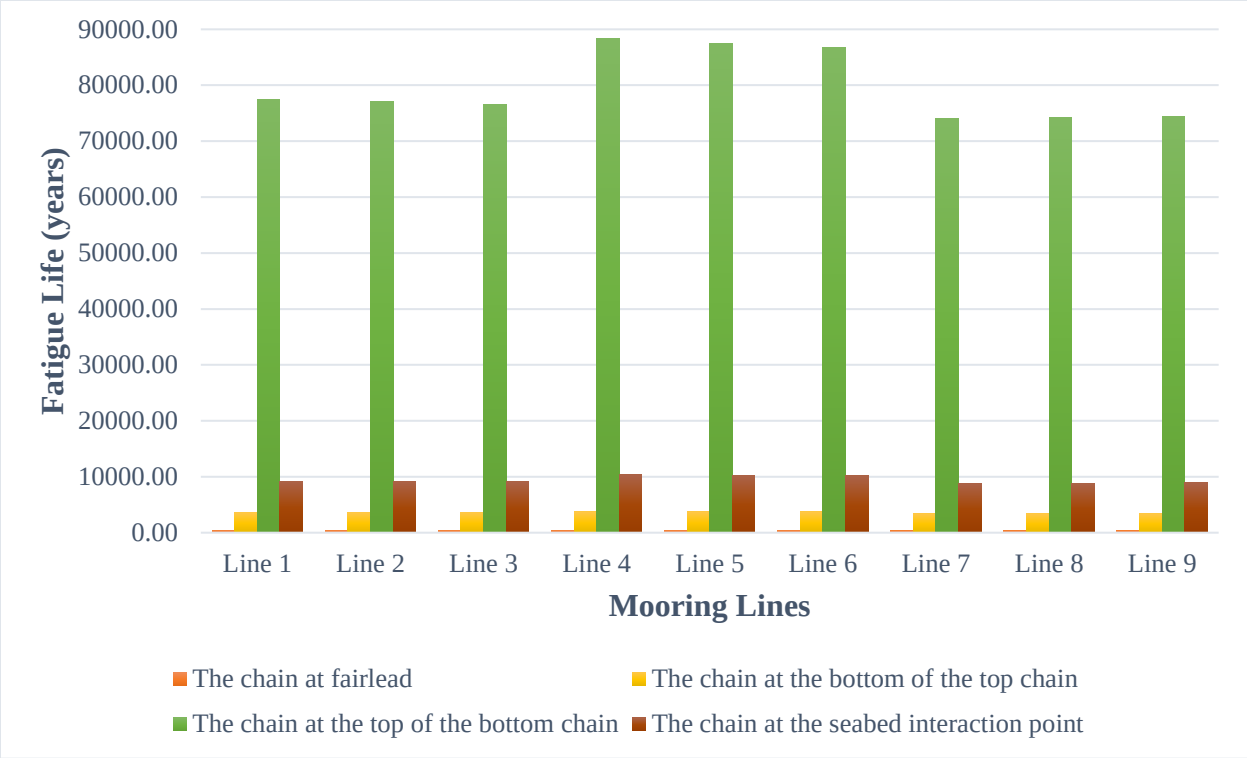

Figure 7-6 The fatigue life considering the combined LF and WF motions for case 1

When considering the combined LF and WF responses, Figure 7-5 indicates that the chain at the fairlead is the most critical location of all the mooring lines. Lines 7 to 9 have the most significant fatigue damage of 0.0030 per year, with line 9 having the shortest fatigue life of 331.75 years. Lines 1 to 6 have 0.0027 fatigue damage per year, while line 6 has the most extended fatigue life of 366.50 years. The figure also shows that combined responses have zero fatigue damage at the chain at the top of the bottom chain.

Furthermore, Figure 7-6 implies that the fatigue life caused by the combined responses is 0.5% more than the LF motion. Thus, no significant difference between the two results. However, the WF response causes more significant damage than LF and combined responses.

7.2 Case 2: chain-polyester-chain system

The second case study comprises a chain-polyester-chain system. First, the chain from the fairlead is 300 m, followed by a polyester rope with 300 m, and finally a chain 400 m long. The chain is generally placed at the bottom as it is abrasion-resistant.

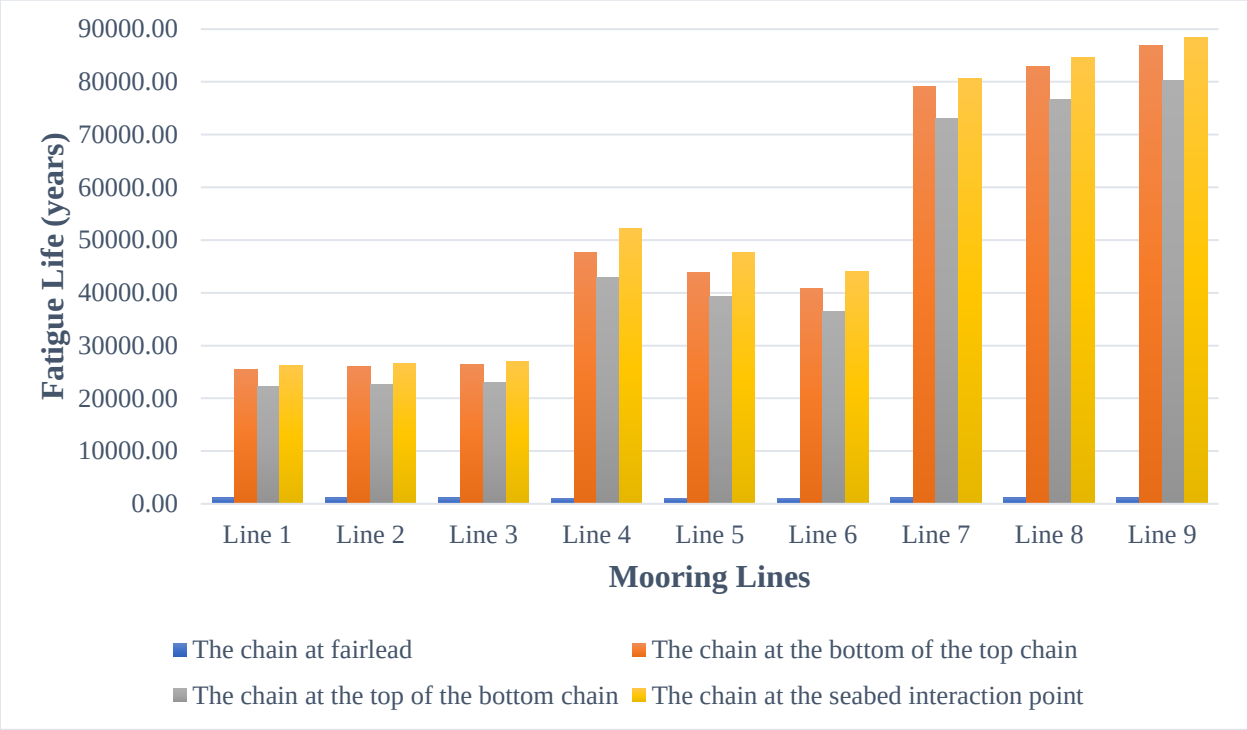

Figure 7-7 The fatigue life caused by LF motion for case 2

The LF motion causes fatigue damage of 0.0009 yearly to the chain at the fairlead for all mooring lines, causing it the most critical fatigue location of the chain-polyester-chain system. In addition, the LF response has no fatigue damage on the other parts of the mooring line.

Figure 7-7 reveals that the fatigue life of the mooring system has drastically increased triple times than in case 1. The shortest fatigue life is 1088.75, the chain at the fairlead. Contrarily, the seabed interaction point chain has the longest fatigue life of 88,460.45 years. The figure also implies that lines 4 to 6 are the critical ones having 1092.45, 1088.75, and 1092.47 years, respectively. The results for LF motion are three times more than in case 1.

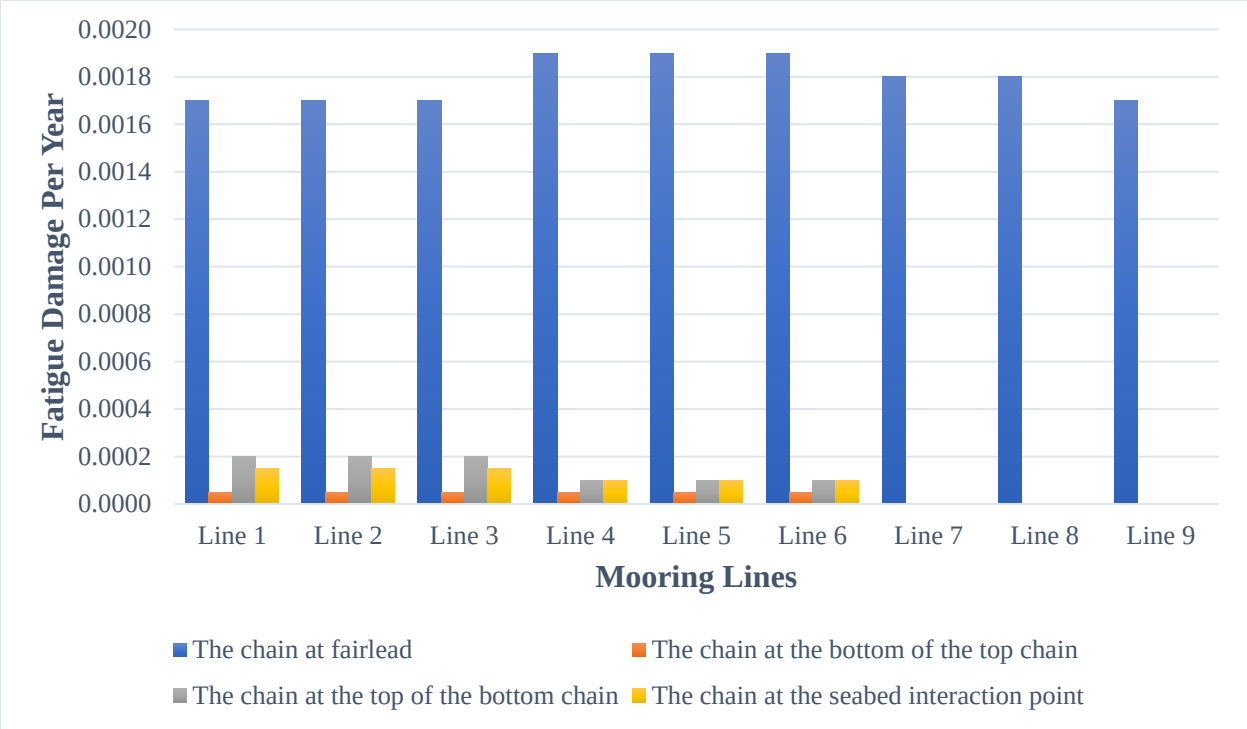

Figure 7-8 The fatigue damage caused by WF motion for case 2

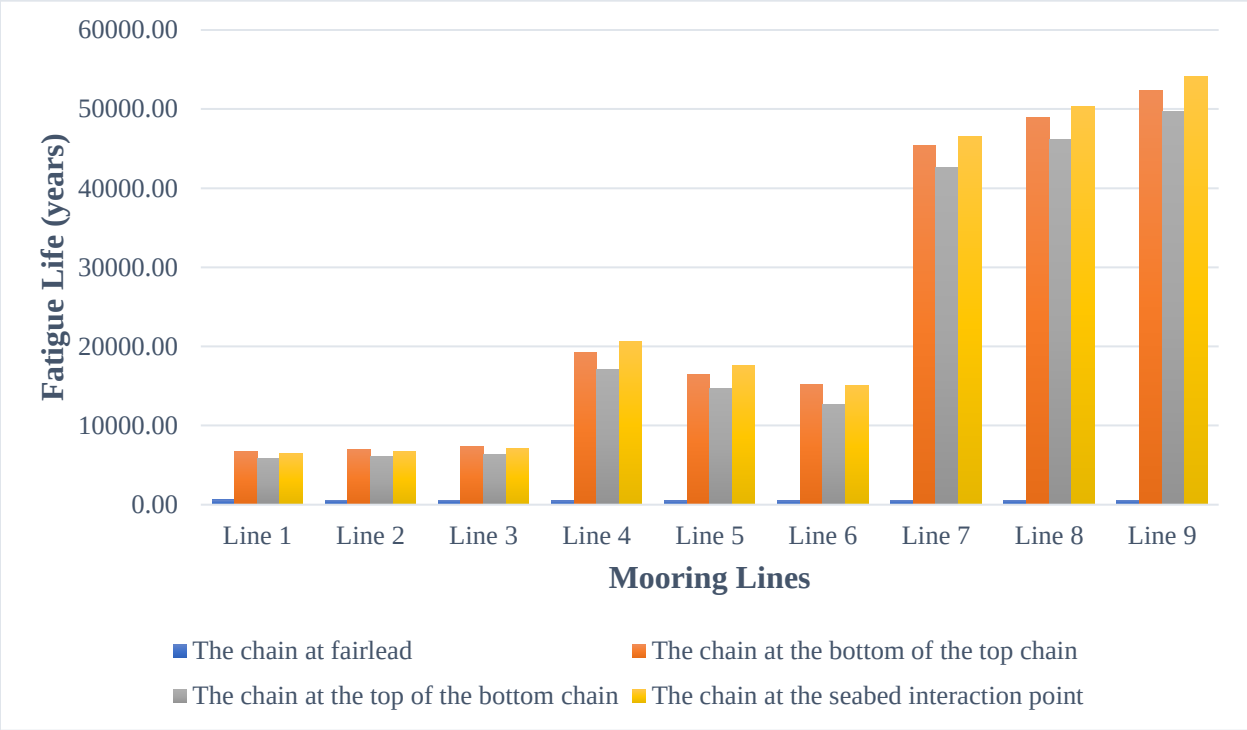

Figure 7-9 The fatigue life caused by WF motion for case 2

The wave response creates fatigue damage on the fairlead chain of 0.0019 every year to lines 4, 5, and 6, as interpreted in Figure 7-8. Lines 7 and 8 have 0.0018 fatigue damage per year, while lines

1, 2, 3, and 9 have 0.0017. Apart from the chain at the fairlead, the figure shows that WF motions generate minimal damage to the other fatigue locations on lines 1 to 6, while lines 7 to 9 have zero fatigue damage. Figure 7-9 shows a 50% difference from the LF motion results.

The chain at the fairlead is the critical fatigue location of the mooring lines due to WF motion. Line 6 has the lowest fatigue life of 528.10 years. However, the most extended fatigue life is line 1, having 596.60 years, approximately 11.50% more than line 6.

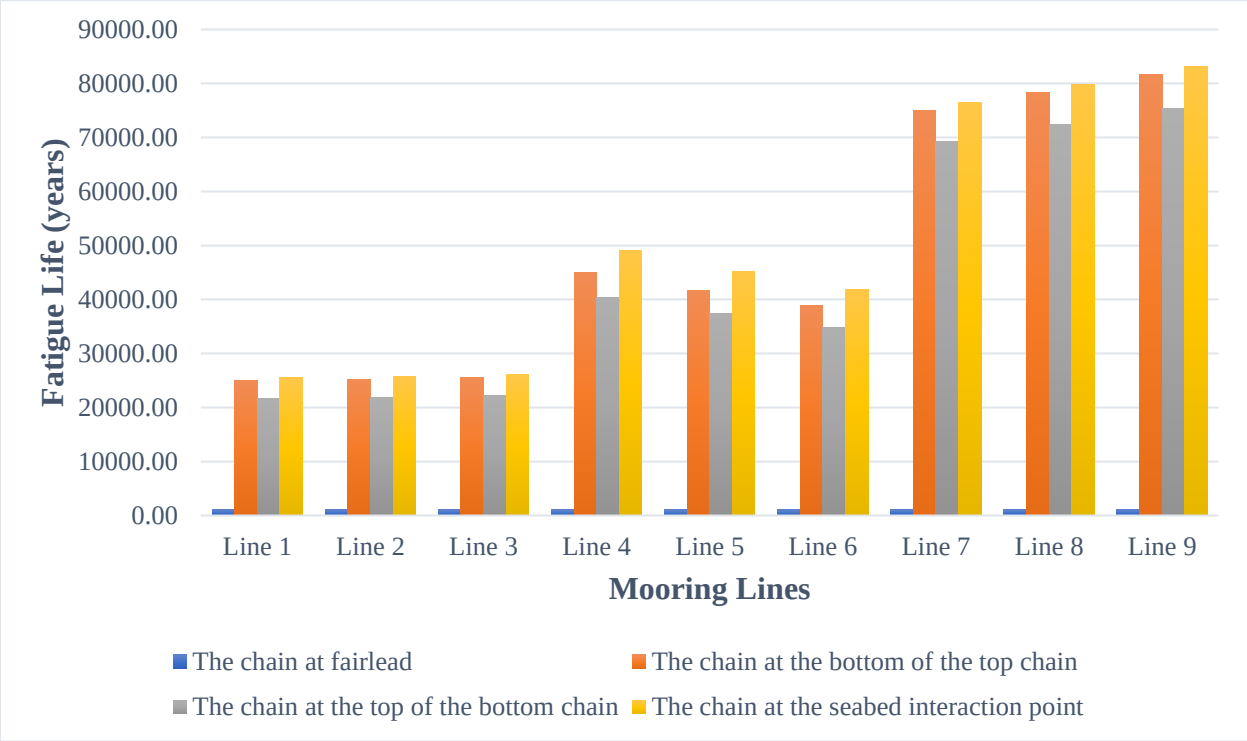

Figure 7-10 The fatigue life caused by the combined LF and WF motions for case 2

The combination of LF and WF motions causes 0.0009 fatigue damage only on the chain at the fairlead of the mooring lines. Figure 7-10 shows that line 5 has 1057.22 fatigue years, making it the most critical one, and line 1 has the longest fatigue life of 1107.07 years.

7.3 Case 3: chain-wire-chain system

The third case has a chain-wire-chain system. All mooring lines are 1000 meters long. The chain from the fairlead is 300 meters, followed by a wire rope with 300 meters, and then a 400-meter chain attached to the anchor. This system offers a higher restoring force and a reduced pre-tension of the mooring lines.

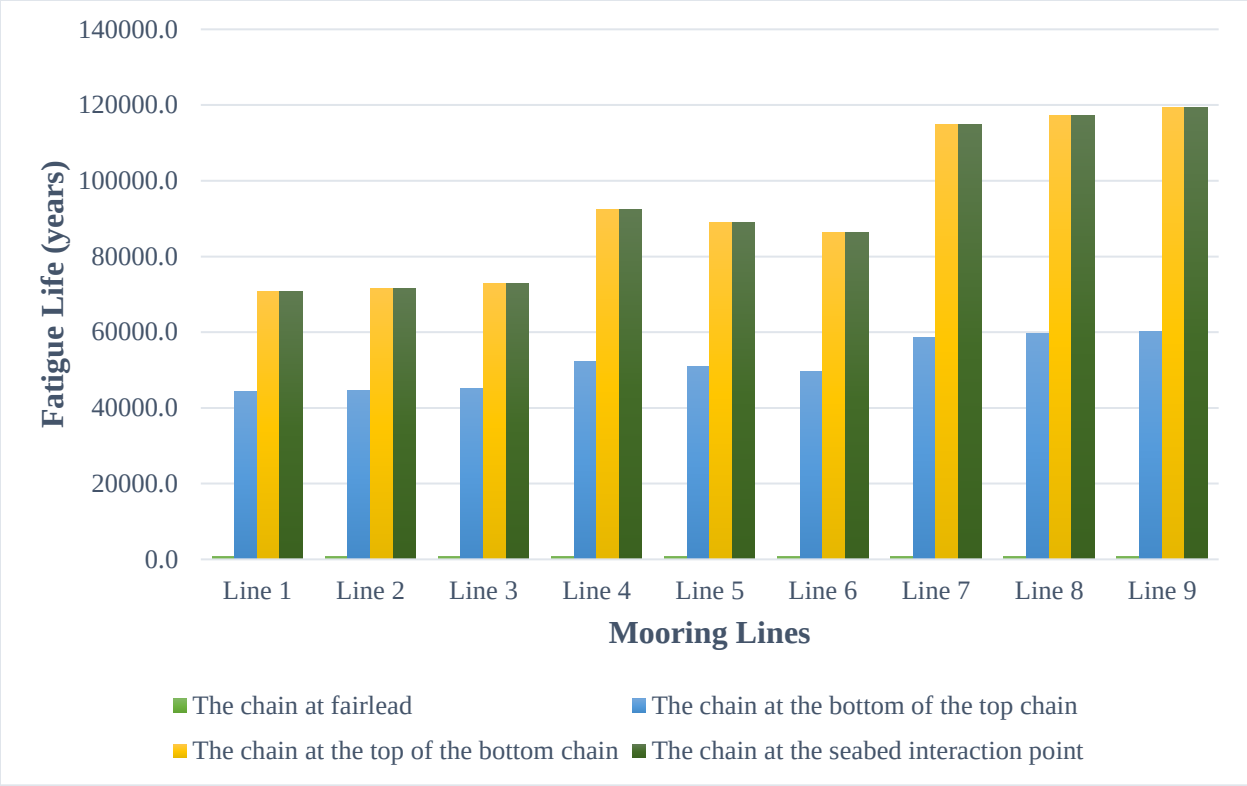

Figure 7-11 The fatigue life caused by LF response for case 3

Results indicate that the chain-wire-chain system is susceptible to LF response causing 0.0012 fatigue damage per year to the chain at fairlead only. That means that other parts of the chain have no fatigue damage. Line 7 has the shortest fatigue life of 832.73 years, while line 6 has the longest fatigue life of 857.08 years, as shown in Figure 7-11. The results are 200% more than case 1 but 26% less than case 2.

Furthermore, Figure 7-11 also shows that the chains at the top of the bottom chain and the seabed interaction point have the same fatigue life. That means that the whole length of the bottom chain is lying on the seabed. Therefore, the wear and corrosion must be considered as it permanently changes the cross-section of the chain. As a result, the fatigue life of the mooring lines is reduced.

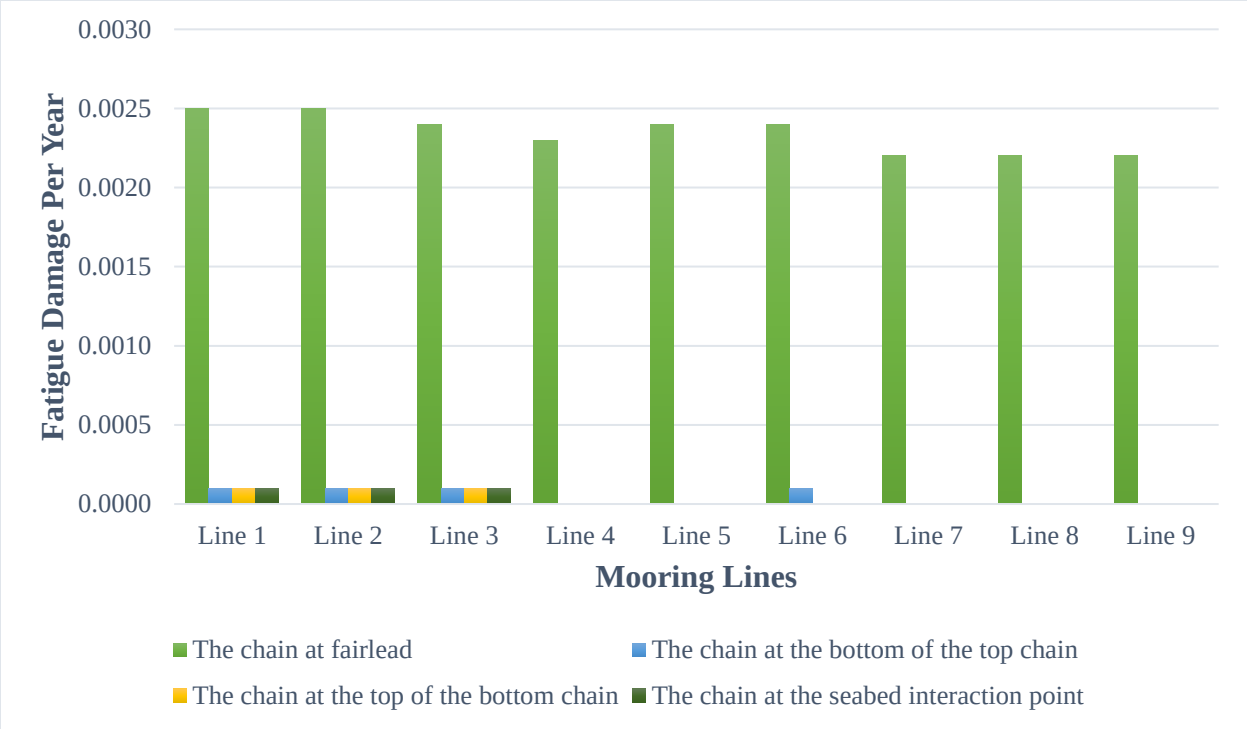

Figure 7-12 The fatigue damage caused by WF response for case 3

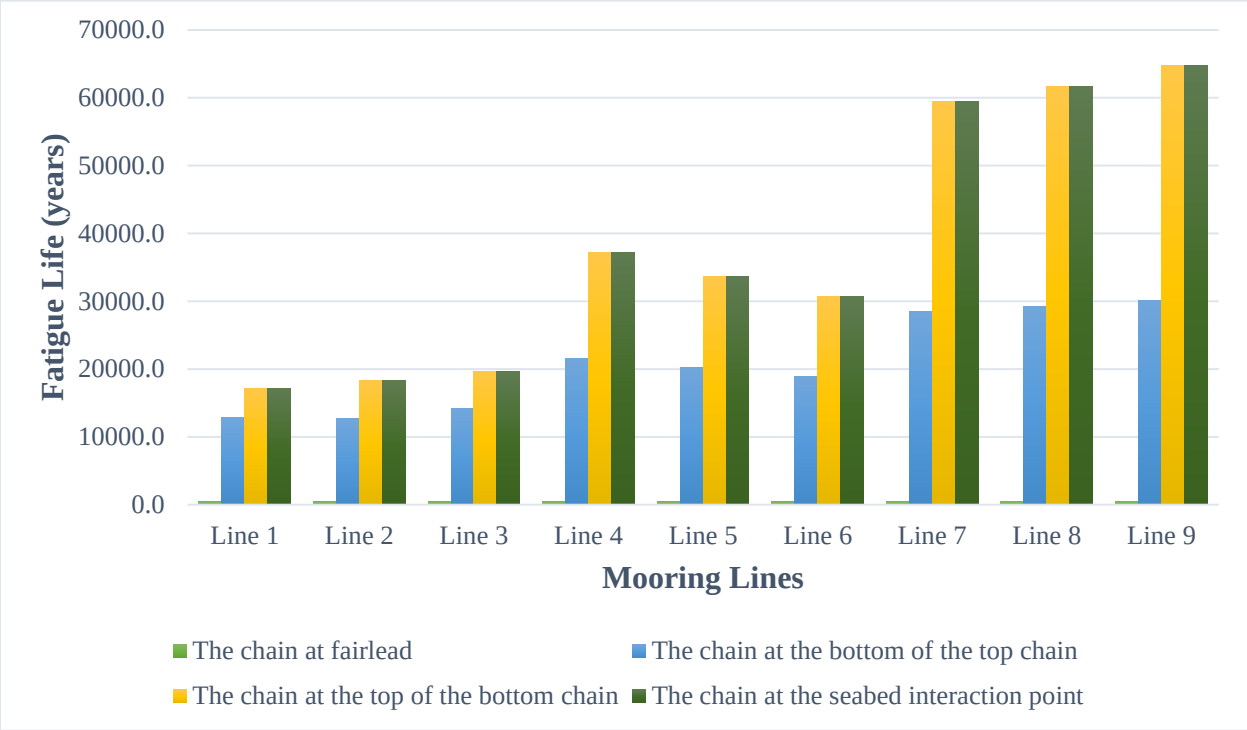

Figure 7-13 The fatigue life caused by WF response for case 3

Like the other two cases, the WF response generates yearly fatigue damage to the chains at the fairlead. Lines 1 and 2 have 0.0025, lines 3, 5, and 6 have 0.0024, line 4 has 0.0023, and lines 7 to

9 have 0.0022 fatigue damage at fairlead, presented in Figure 7-12. The figure also shows that lines 1 to 3 have equal damage of 0.0001 on other parts of the line. However, there is no observed fatigue damage on lines 4 to 5 and 7 to 9.

Figure 7-13 proves the viscous damping of the mooring lines as the deterioration starts from the fairlead down to the bottom chain at the anchoring point. Line 1 appears to have the shortest fatigue life of 402.88 years, which is more than half of the fatigue life caused by LF motion. It manifests that the WF response creates more damage than the LF response.

Moreover, the longest fatigue life occurs at line 9, having 459.58 years. The chain at the bottom of the top chain of the lines has a fatigue life ranging from 12,800 to 30,200 years. Also, the chain at the top of the bottom chain ranges from 17,100 to 64,800 fatigue years.

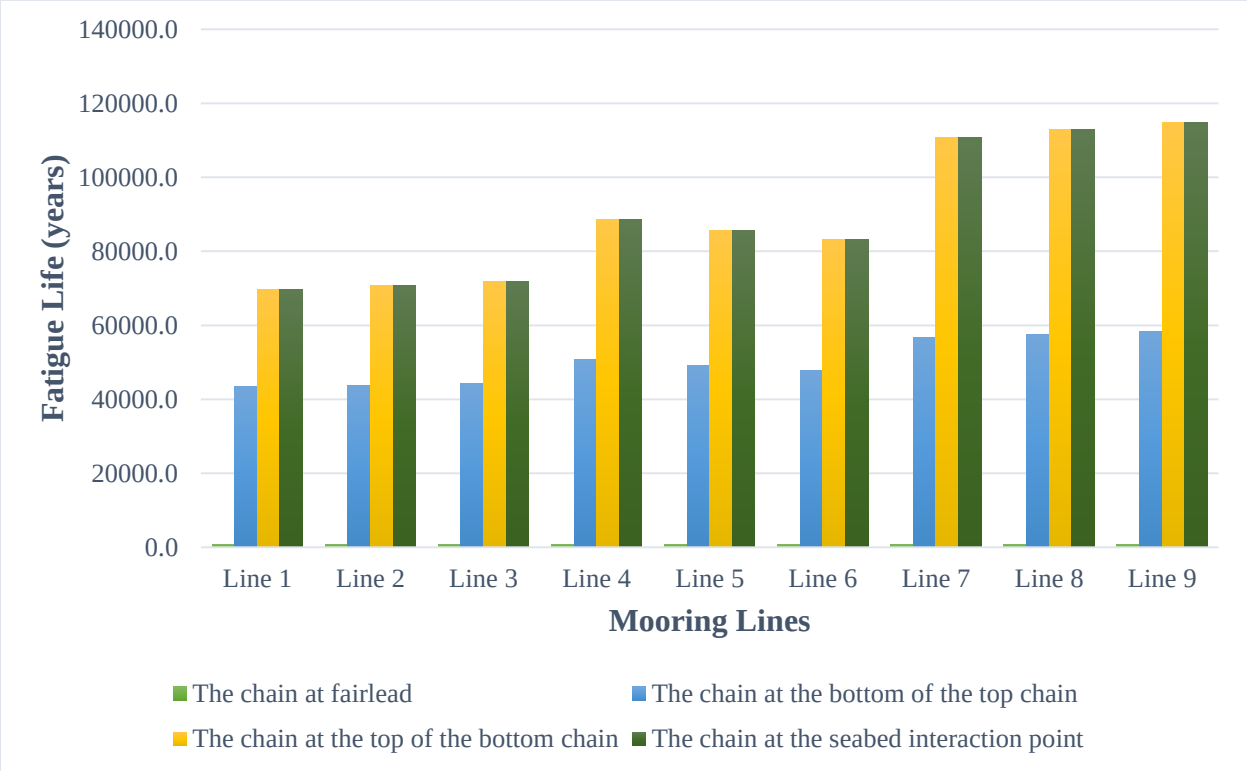

Figure 7-14 The fatigue life caused by the combined LF and WF responses for case 3

The combined LF and WF responses create 0.0012 fatigue damage to the chains at fairlead of all the mooring lines. However, it must be noted that the combined responses for cases 2 and 3 significantly damage the chain at the fairlead only. Thus, a massive difference between the fatigue life of the fairlead chain and the other fatigue locations is distinguishable. Furthermore, the shortest

fatigue life occurs in line 8 with 814.68 years, while line 1 has the most extended fatigue life of 838.75 years, as presented in Figure 7-14. The chain at the seabed interaction point is consistently the least critical fatigue location among the mooring lines.

Chapter 8 Summary and Conclusions

The summary and conclusions are presented in this chapter. In addition, the suggestions for further research are also discussed due to the limitations of this study.

8.1 Summary

An in-depth study of the mooring systems and fatigue analysis is the core of this master thesis. It consists of a literature review and case studies.

The mooring system serves as station-keeping for the floating structures while performing offshore activities under unfavourable environmental conditions. Furthermore, mooring systems are subjected to fluctuating stresses due to environmental factors resulting in fatigue damage. Studies show that fatigue is one of the primary reasons mooring lines fail. Thus, it plays a vital role in the design and analysis of the mooring system. Furthermore, research reveals that the fairlead chain is often the most critical fatigue location of the mooring line. Accordingly, the mooring system's life depends on the chain's fatigue life at fairlead, as it bears the shortest fatigue life. For this reason, most studies only conduct a local fatigue analysis focusing on the upper chain of the mooring lines. Therefore, this master thesis aims to perform global fatigue analysis of mooring systems, particularly of a turret moored FPSO with GOM metocean conditions.

A brief overview of the floating offshore structures and riser systems is presented in this paper. The environmental loads and conditions are also discussed thoroughly. Furthermore, three cases of different mooring systems have been established to analyse further the global fatigue analysis of the mooring lines induced by LF, WF, and combined responses.

The OrcaFlex software performs static, dynamic, and fatigue analyses of the mooring systems. The water depth used is 400 meters. The mooring system is composed of nine mooring lines divided into three clusters. The chain-chain-chain, chain-polyester-chain, and chain-wire-chain systems are studied in this paper.

8.2 Conclusions

The following conclusions are drawn derived from the observed results.

1. The chain at fairleads is the most critical fatigue location of the mooring lines when considering the LF, WF, and combined responses. Conversely, the least critical fatigue location is the chain at the top of the bottom chain in case 1, while it is the chain at the seabed interaction point in cases 2 and 3.
2. The LF and the combined responses cause similar fatigue damage to the mooring lines, resulting in a 0.5% deviation of the fatigue life.
3. The WF response generates more serious fatigue damage by approximately 23%, 47%, and 52% in case 1, case 2, and case 3, respectively, than LF and combined responses.
4. The fatigue life induced by WF motion is roughly 50% less than the LF and combined motions.
5. The fatigue life of the chain-polyester-chain system is three times more than the chain-chain-chain system and 25% more than the chain-wire-chain system. Therefore, the chain-polyester-chain is the best mooring system among the three cases.
6. This study validates the proposition of Wu et al. [1] that mooring configurations, layout, platform types, and metocean parameters affect the fatigue locations of the mooring lines.

8.3 Suggestions for Future Work

This study mainly focuses on the mooring systems of the FPSO. Thus, future researchers may perform a global fatigue analysis with the riser system to see if the fatigue life of the mooring system is reduced or increased. In addition, other directions of the wave, current, and wind must also be considered. The use of other types of offshore floating structures is also a possibility.

References

[1] Y. Wu, T. Wang, Ø. Eide and K. Haverty, Governing Factors and Locations of Fatigue Damage on Mooring Lines, Ocean Engineering, vol. 96, 2015, pp. 109-124.

[2] L. Keshavarz, Analysis of Mooring System for a Floating Production System, Trondheim: Norwegian University of Science and Technology, 2011, p. 1.

[3] K.-T. Ma, Y. Luo, T. Kwan and Y. Wu, Mooring System Engineering for Offshore Structures, Elsevier Inc., 2019.

[4] J. Halkyard, "Floating Offshore Platform Design," in *Handbook of Offshore Engineering*, S. Chakrabarti, Ed., Elsevier, 2005, pp. 419-661.

[5] A. Reza and H. Sedighi, "Nonlinear Vertical Vibration of Tension Leg Platforms with Homotopy Analysis Method," *Advances in Applied Mathematics and Mechanics*, vol. 7, 2014.

[6] *Introduction to Spars.* [Film]. Technip.

[7] M. F. H. Faddzal, "Experimental Studies on the Optimum Configuration of Mooring Line for Truss Spar Platform," 2015.

[8] API RP 2SK, Recommended Practice for Design and Analysis of Stationkeeping Systems for Floating Structures, Washington: American Petroleum Institute, 2005, pp. 16, 59-60.

[9] N. K. Mitra, Fundamentals of Floating Production Systems, Allied Publishers Private Limited, 2009.

[10] E. Mulford and J. Cabrera, "Methodology for the Experimental Analysis of Offshore System in Deep and Ultra-Deep Waters in the Colombia Caribbean Sea," *Ship Science & Technology*, 2018.

[11] MODEC, Inc, "https://www.modec.com/," [Online].

[12] E. Mollaahmetoğlu and A. Mentes, "Floating Production Storage and Offloading Units and Topside Facilities," 2019.

[13] W. Mueller, "How FPSO Motion Affect Separator Performance, Controls," *Oil & Gas Journal*, 1997.

[14] DNVGL-OS-E301, Offshore Standards for Position Mooring, Oslo: Det Norske Veritas AS, 2018, pp. 12, 22.

[15] ABC Moorings, "http://abc-moorings.weebly.com/," [Online].

[16] K. Wåsjø, T. Böllmann and H. Andersen, K12 - Design of Mooring and Anchoring, Statens vegvesen, 2019.

[17] OTEC Moorings Inc, "https://sites.google.com/site/otecmooringsinc/," [Online].

[18] The Centre for Marine and Petroleum Technology, Floating Structures: A Guide for Design and Analysis, vol. 2, N. Barltrop, Ed., Oilfield Publications Limited.

[19] D. Brown, "Mooring Systems," in *Handbook of Offshore Engineering*, S. Chakrabarti, Ed., Elsevier, 2005, pp. 663-706.

[20] DNVGL-OS-E302, Offshore Standards for Offshore Mooring Chain, Oslo: Det Norske Veritas AS, 2018.

[21] Vryhof Anchors B.V., Vryhof Manual: The Guide to Anchoring, 2015.

[22] DNVGL-OS-E304, Offshore Standard for Offshore Mooring Steel Wire Ropes, Oslo: Det Norske Veritas AS, 2015.

[23] API RP 2SM, Recommended Practice for Design, Manufacture, Installation, and Maintenance of Synthetic Fiber Ropes for Offshore Mooring, Washington: American Petroleum Institute, 2001.

[24] Y. Bai and Q. Bai, "Design of Deepwater Risers," in *Subsea Pipelines and Risers*, Elsevier Science Ltd, 2005, pp. 401-412.

[25] DNVGL-SE-0476, Service Specification for Offshore Riser Systems, Oslo: Det Norske Veritas AS, 2017.

[26] D. Drubers, Wet Collapse Behavior of Flexible UDW Risers, Delft: Delft University of Technology, 2018.

[27] K.-S. Kim, H.-S. Choi and K. S. Kim, "Preliminary Optimal Configuration on Free Standing Hybrid Riser," *International Journal of Naval Architecture and Ocean Engineering*, vol. 10, no. 3, pp. 250-258, 2018.

[28] S. Siriwardane, Module 4-1: Theoretical Basis of Fatigue: FLS of Steel Structures, Lecture Notes, Stavanger, 2021.

[29] Orcina Ltd., OrcaFlex Help 11.0g, 2021.

[30] The Centre for Marine and Petroleum Technology, Floating Structures: A Guide for Design and Analysis, vol. 1, N. Barltrop, Ed., Oilfield Publications Limited.

[31] DNV-RP-C205, Recommended Practice for Environmental Conditions and Environmental Loads, Oslo: Det Norske Veritas AS, 2014, p. 18.

[32] DNVGL-CG-0130, Class Guideline for Wave Loads, Oslo: Det Norske Veritas AS, 2018, p. 47.

[33] J. Mendoza, P. Haagensen and J. Köhler, "Analysis of Fatigue Test Data of Retrieved Mooring Chain Links Subject to Pitting Corrosion," in *Marine Structures*, vol. 81, 2022.

Appendices

Appendix A – The Tabulated Fatigue Life of The Moorings

The fatigue life of the chain at fairlead (years)									
Mooring	Case 1			Case 2			Case3		
	LF	WF	Combined	LF	WF	Combined	LF	WF	Combined
Line 1	365.81	282.19	366.17	1152.33	596.60	1107.07	854.89	402.88	838.75
Line 2	364.83	281.24	365.30	1144.11	590.53	1098.83	853.09	406.6	838.03
Line 3	363.51	280.13	364.27	1133.37	586.89	1087.62	852.38	410.26	836.45
Line 4	364.17	274.59	363.73	1092.45	529.02	1059.10	855.37	426.61	831.87
Line 5	365.02	275.04	365.34	1088.75	529.02	1057.22	855.79	422.74	834.85
Line 6	364.58	276.25	366.50	1092.47	528.10	1063.53	857.08	418.52	834.68
Line 7	332.45	261.45	331.84	1120.33	567.16	1081.33	832.73	458.50	815.09
Line 8	332.21	261.26	331.98	1125.61	570.83	1084.87	834.14	458.91	814.68
Line 9	331.79	260.61	331.75	1129.66	573.16	1089.05	834.73	459.58	815.82

The fatigue life of the chain at the bottom of the top chain (years)									
Mooring	Case 1			Case 2			Case3		
	LF	WF	Combined	LF	WF	Combined	LF	WF	Combined
Line 1	3583.35	2540.94	3607.93	25523.01	6697.88	24926.63	44277.13	12840.01	43357.11
Line 2	3590.22	2539.82	3614.35	25947.09	6955.68	25274.42	44719.59	12654.86	43800.04
Line 3	3601.39	2535.74	3629.14	26367.17	7301.25	25612.94	45049.12	14122.24	44240.46
Line 4	3736.88	2764.16	3739.06	47572.39	19233.60	44996.43	52312.68	21568.04	50649.9
Line 5	3715.86	2732.37	3726.90	43921.86	16426.17	41746.82	51001.21	20254.44	49233.09
Line 6	3692.71	2703.69	3715.61	40832.81	15254.08	38973.62	49650.99	18877.4	47884.63
Line 7	3382.68	2652.46	3409.20	79171.79	45453.91	75035.48	58626.28	28438.94	56649.03
Line 8	3385.06	2657.88	3410.79	82911.74	48996.99	78301.26	59558.27	29183.83	57470.43
Line 9	3398.50	2679.80	3412.77	86866.82	52299.86	81592.62	60304.43	30164.15	58189.90

The fatigue life of the chain at the top of the bottom chain (years)									
Mooring	Case 1			Case 2			Case3		
	LF	WF	Combined	LF	WF	Combined	LF	WF	Combined
Line 1	76330.62	50022.34	77497.32	22339.89	5842.97	21629.96	70807.32	17192.88	69716.28
Line 2	76877.85	49789.23	77107.00	22641.91	6074.18	21864.71	71567.65	18350.79	70861.31
Line 3	76630.87	49768.10	76509.73	22957.54	6339.42	22165.41	72798.71	19581.63	71945.09
Line 4	86779.73	62625.68	88348.91	42833.43	17088.80	40362.17	92415.02	37179.53	88575.59
Line 5	86227.82	62788.22	87383.49	39256.59	14653.73	37356.90	88973.23	33639.16	85663.12
Line 6	85317.76	62383.89	86731.22	36385.49	12697.05	34752.82	86273.6	30739.81	83310.87
Line 7	74201.44	58141.49	74061.91	73063.61	42571.40	69292.40	114878.13	59485.44	110861.77
Line 8	74083.77	59471.50	74205.99	76714.78	46123.22	72382.48	117250.34	61721.76	112866.61
Line 9	74423.29	61224.32	74340.71	80178.87	49667.37	75343.56	119243.76	64732.52	114725.59

Appendices

The fatigue life of the chain at the seabed interaction point (years)									
Mooring	Case 1			Case 2			Case3		
	LF	WF	Combined	LF	WF	Combined	LF	WF	Combined
Line 1	9110.74	6725.78	9220.37	26283.64	6440.19	25476.02	70807.32	17192.88	69716.28
Line 2	9151.99	6679.74	9190.19	26661.78	6731.66	25777.22	71567.65	18350.79	70861.31
Line 3	9122.25	6663.10	9107.86	27072.64	7068.92	26169.37	72798.71	19581.63	71945.09
Line 4	10188.53	7048.41	10361.33	52199.13	20672.04	49066.73	92415.02	37179.53	88575.59
Line 5	10123.29	7625.82	10264.20	47591.53	17579.43	45248.13	88973.23	33639.16	85663.12
Line 6	10029.61	7577.48	10187.69	43956.18	15053.23	41939.66	86273.6	30739.81	83310.87
Line 7	8851.64	6353.83	8820.13	80570.09	46484.13	76407.35	114878.13	59485.44	110861.77
Line 8	8876.55	6485.10	8879.48	84619.84	50279.77	79797.96	117250.34	61721.76	112866.61
Line 9	8919.86	6640.83	8924.93	88460.45	54130.55	83092.83	119243.76	64732.52	114725.59

Appendix B – The Tabulated Fatigue Damage of the Moorings

Fatigue damage of the chain at fairlead (per year)									
Mooring	Case 1			Case 2			Case3		
	LF	WF	Combined	LF	WF	Combined	LF	WF	Combined
Line 1	0.0027	0.0035	0.0027	0.0009	0.0017	0.0009	0.0012	0.0025	0.0012
Line 2	0.0027	0.0036	0.0027	0.0009	0.0017	0.0009	0.0012	0.0025	0.0012
Line 3	0.0028	0.0036	0.0027	0.0009	0.0017	0.0009	0.0012	0.0024	0.0012
Line 4	0.0027	0.0036	0.0027	0.0009	0.0019	0.0009	0.0012	0.0023	0.0012
Line 5	0.0027	0.0036	0.0027	0.0009	0.0019	0.0009	0.0012	0.0024	0.0012
Line 6	0.0027	0.0036	0.0027	0.0009	0.0019	0.0009	0.0012	0.0024	0.0012
Line 7	0.0030	0.0038	0.0030	0.0009	0.0018	0.0009	0.0012	0.0022	0.0012
Line 8	0.0030	0.0038	0.0030	0.0009	0.0018	0.0009	0.0012	0.0022	0.0012
Line 9	0.0030	0.0038	0.0030	0.0009	0.0017	0.0009	0.0012	0.0022	0.0012

Fatigue damage of the chain at the bottom of the top chain (per year)									
Mooring	Case 1			Case 2			Case3		
	LF	WF	Combined	LF	WF	Combined	LF	WF	Combined
Line 1	0.0003	0.0004	0.0003	0.0000	0.0001	0.0000	0.0000	0.0001	0.0000
Line 2	0.0003	0.0004	0.0003	0.0000	0.0001	0.0000	0.0000	0.0001	0.0000
Line 3	0.0003	0.0004	0.0003	0.0000	0.0001	0.0000	0.0000	0.0001	0.0000
Line 4	0.0003	0.0004	0.0003	0.0000	0.0001	0.0000	0.0000	0.0000	0.0000
Line 5	0.0003	0.0004	0.0003	0.0000	0.0001	0.0000	0.0000	0.0000	0.0000
Line 6	0.0003	0.0004	0.0003	0.0000	0.0001	0.0000	0.0000	0.0001	0.0000
Line 7	0.0003	0.0004	0.0003	0.0000	0.0000	0.0000	0.0000	0.0000	0.0000
Line 8	0.0003	0.0004	0.0003	0.0000	0.0000	0.0000	0.0000	0.0000	0.0000
Line 9	0.0003	0.0004	0.0003	0.0000	0.0000	0.0000	0.0000	0.0000	0.0000

Fatigue damage of the chain at the top of the bottom chain (per year)									
Mooring	Case 1			Case 2			Case3		
	LF	WF	Combined	LF	WF	Combined	LF	WF	Combined
Line 1	0.0000	0.0000	0.0000	0.0000	0.0002	0.0000	0.0000	0.0001	0.0000
Line 2	0.0000	0.0001	0.0000	0.0000	0.0002	0.0000	0.0000	0.0001	0.0000
Line 3	0.0000	0.0000	0.0000	0.0000	0.0002	0.0000	0.0000	0.0001	0.0000
Line 4	0.0000	0.0000	0.0000	0.0000	0.0001	0.0000	0.0000	0.0000	0.0000
Line 5	0.0000	0.0000	0.0000	0.0000	0.0001	0.0000	0.0000	0.0000	0.0000
Line 6	0.0000	0.0000	0.0000	0.0000	0.0001	0.0000	0.0000	0.0000	0.0000
Line 7	0.0000	0.0000	0.0000	0.0000	0.0000	0.0000	0.0000	0.0000	0.0000
Line 8	0.0000	0.0000	0.0000	0.0000	0.0000	0.0000	0.0000	0.0000	0.0000
Line 9	0.0000	0.0000	0.0000	0.0000	0.0000	0.0000	0.0000	0.0000	0.0000

Appendices

Fatigue damage of the chain at the seabed interaction point (per year)									
Mooring	Case 1			Case 2			Case3		
	LF	WF	Combined	LF	WF	Combined	LF	WF	Combined
Line 1	0.00010	0.00015	0.00010	0.00000	0.00015	0.00000	0.00000	0.00010	0.00000
Line 2	0.00010	0.00015	0.00010	0.00000	0.00015	0.00000	0.00000	0.00010	0.00000
Line 3	0.00010	0.00015	0.00010	0.00000	0.00015	0.00000	0.00000	0.00010	0.00000
Line 4	0.00010	0.00010	0.00010	0.00000	0.00010	0.00000	0.00000	0.00000	0.00000
Line 5	0.00010	0.00010	0.00010	0.00000	0.00010	0.00000	0.00000	0.00000	0.00000
Line 6	0.00010	0.00010	0.00010	0.00000	0.00010	0.00000	0.00000	0.00000	0.00000
Line 7	0.00010	0.00015	0.00010	0.00000	0.00000	0.00000	0.00000	0.00000	0.00000
Line 8	0.00010	0.00015	0.00010	0.00000	0.00000	0.00000	0.00000	0.00000	0.00000
Line 9	0.00010	0.00015	0.00010	0.00000	0.00000	0.00000	0.00000	0.00000	0.00000